THEORIES, CONSTRUCTION, AND APPLICATIONS OF THE WATER TABLE

HOWARD LEE SMOLIN
ROBERT ALTON THOMPSON

THEORY, CONSTRUCTION, AND APPLICATIONS OF THE WATER TABLE

BY

LCDR HOWARD LEE SMOLIN, USN

AND

LCDR ROBERT ALTON THOMPSON, USN

SUBMITTED TO THE FACULTY OF THE RENSSELAER POLYTECHNIC INSTITUTE IN PARTIAL FULFILLMENT OF THE REQUIREMENTS FOR THE DEGREE OF MASTER OF SCIENCE

TROY, NEW YORK JUNE 11,1947

TABLE OF CONTENTS

ACKNOWLEDGMENT

The work herein presented was done under the supervision and guidance of Professor Neil P. Bailey, Head of the Department of Mechanical Engineering at the Rensselaer Polytechnic Institute. The writers wish to express their appreciation for the timely suggestions and aid offered by Professor Bailey, and for the assistance tendered by Professors C. K. Palsgrove, J. J. Devine, and H. A. Wilson, all of the Mechanical Engineering Department at the Rensselaer Polytechnic Institute. The writers would also like to express their thanks to Mr. F. H. Johnson and Mr. W. Miles, of the General Electric Company, Schenectady, New York, for their suggestions and support.

ABSTRACT

The object of this thesis is threefold, to present the theoretical analogy between the flow of a compressible gas, such as air, and the flow of water with a free surface, to describe the details of construction of the water table which utilizes the above analogy, and to outline and demonstrate the applications of the water table in the investigation of air flow.

The analogy between air flow and water with a free surface is presented in Part I. Part II contains a description in detail of the construction of the water table at the Rensselaer Polytechnic Institute. The applications of the water table and one demonstration of its use are found in Part III.

This work was done during the months of February through May 1947 at the Rensselaer Polytechnic Institute.

NOMENCLATURE

The following nomenclature is used in this paper:

AIR

C_p = specific heat at constant pressure, Btu per lb per deg F

C_v = specific heat at constant volume, Btu per lb per deg F

d = total differential

∂ = partial differential

g = acceleration of gravity; 32.1 fps per sec

J = 778.26 ft-lb per Btu

L = mechanical work, Btu per lb

P = pressure, psfa

Q = heat added, Btu per lb

R = gas constant; 53.3 for air

T = absolute static temperature, deg Rankine

V = specific volume; cu ft per lb

v = velocity, fps

v_g^* = velocity of a sound wave, fps

v_{max} = maximum velocity

W = weight flow, lb per sec

γ = ratio of gas specific heats, C_p/C_v ; 1.395 for cold air

ρ = mass density, slugs per cu ft

NOMENCLATURE

The following nomenclature is used in this paper:

WATER

a,b,c = components of the velocity in the x,y,z directions

h = water depth, ft

h_o = total head (water depth when v=0), ft

h_o' = total head after hydraulic jump, ft

p = pressure, psfa

Q = quantity of flow, cu ft per sec

v = velocity, fps

v_s^* = velocity of propogation of a surface wave, fps

v_{max} = maximum velocity

x,y,z = rectangular coordinates in flow space

o, p_o, T_o = stagnation state (subscript "o")

ρ = mass density, slugs per cu ft

INTRODUCTION

The operation of a supersonic wind tunnel for test work at transsonic and supersonic air speeds is an expensive project, requiring costly equipment, elaborate instrumentation, and an enormous amount of power. A sizeable staff of skilled technicians and much time are needed in the fabrication of models to be used in the tunnel and in the actual operation and maintenance of the tunnel and its adjuncts.

The reduction in the amount of test work that must be done in high velocity air would save a considerable amount of time and expense. This would facilitate design, experimentation, and theoretical research in the field of high velocity airflow.

It is the intent of this paper to show that the water table may be advantageously employed in conjunction with the wind tunnel. Its use for preliminary work would replace, to a considerable extent, the operations necessary in the wind tunnel.

The work herein presented was undertaken with three primary objectives in mind: (1) an investigation of the existing theoretical analogy between the two dimensional flow of a compressible gas, such as air, and the flow of shallow water with a free surface, (2) the construction of a water table, a device designed to utilize the flow analogy, and (3) an investigation of the flow around a few basic models in order to check the analogy with existing air flow theory and to demonstrate the usefulness of the water table.

By a comparison of the energy and continuity equations for two dimensional gas flow and water flow with a free surface, it was found that an analogy exists between the ratio of absolute air temperatures and water depth ratio, the ratio of gas densities and water depth ratio, and the ratio of gas pressures and the square of the water depth ratio. This analogy is quantitatevly correct for a fictitious gas having a $= C_p/C_v$ of 2.0. "Hydraulic jump" in water flow is used to represent "compression shock" in air flow.

In order to demonstrate the usefulness of the water table as applied to the study of supersonic air flow, it was originally intended to check a few of the existing principles of supersonic air flow theory on the water table. Experiments were also proposed to investigate that part of high velocity air flow about which little is known at present. Due to difficulties encountered in the construction of the water table, little time was available for model construction and test work. Therefore, only one application of the water table is presented. This is an investigation of high velocity flow around a fifteen degree wedge.

This work was done during the months of February through May 1947 at the Rensselaer Polytechnic Institute. The water table was constructed in the Mechanical Engineering Laboratory of the Rensselaer Polytechnic Institute.

PART I

THE WATER ANALOGY OF SUPERSONIC AIR FLOW

Reversibility, in the case of a compressible fluid such as air, is defined by the statement that the change in internal energy ($C_v dT$) is caused entirely by expansion or compression work ($\frac{1}{J}PdV$) or

$$J(C_v dT) + PdV = 0 \qquad (1)$$

The state of a compressible fluid is defined by the gas equation:

$$PV = RT \qquad (2)$$

If the gas equation (2) is differentiated we have:

$$PdV + VdP = RdT$$

and since, at any instant, $V = \frac{RT}{P}$, then

$$PdV + RT\frac{dP}{P} = RdT$$

or

$$PdV = RdT - RT\frac{dP}{P} \qquad (3)$$

Substituting this value for PdV in equation (1):

$$J(C_v + \frac{R}{J})dT = RT\frac{dP}{P} \qquad (4)$$

but

$$C_v + \frac{R}{J} = C_p = \frac{\gamma}{\gamma-1}\frac{R}{J} \quad \text{where} \quad \gamma = \frac{C_p}{C_v}$$

Then equation (4) becomes:

$$\frac{\gamma}{\gamma-1}\,dT = T\frac{dP}{P}$$

or

$$\frac{dT}{T} = \frac{\gamma-1}{\gamma}\frac{dP}{P} \qquad (5)$$

Integrating (5) gives:

$$\frac{T}{T_o} = \left(\frac{P}{P_o}\right)^{\frac{\gamma-1}{\gamma}}$$

or

$$\frac{P}{P_o} = \left(\frac{T}{T_o}\right)^{\frac{\gamma}{\gamma-1}} \qquad (6)$$

From the gas equation, using (W) pounds of air:

$$PV = WRT$$

or

$$P = \rho gRT \qquad (7)$$

Using this P in equation (6) gives:

$$\frac{\rho}{\rho_o}\frac{T}{T_o} = \left(\frac{T}{T_o}\right)^{\frac{\gamma}{\gamma-1}}$$

Then:

$$\frac{\rho}{\rho_o} = \left(\frac{T}{T_o}\right)^{\frac{1}{\gamma-1}} \qquad (8)$$

By combining equations (6) and (8):

$$\frac{P}{P_o} = \left(\frac{\rho}{\rho_o}\right)^{\gamma} \qquad (9)$$

Equations (6), (8), and (9) define the relationships between P, ρ, and T for compressible gas flow which is reversible (no heat added and no friction).

The general energy equation for gas flow:

$$dQ + dL = C_v dT + \frac{1}{J}PdV + \frac{1}{J}VdP + \frac{1}{Jg}vdv$$

For the case of no heat added and no outside work done on the gas (dQ = 0, dL = 0):

$$C_v dT + \frac{1}{J}PdV + \frac{1}{J}VdP + \frac{1}{Jg}vdv = 0$$

but

$$C_v dT + \frac{1}{J}PdV + \frac{1}{J}VdP = C_p dT$$

Then:

$$C_p dT + \frac{1}{Jg}vdv = 0 \qquad (10)$$

Integrating between the limits of T_o and T:

$$C_p(T_o - T) = -\frac{1}{2Jg}(v_o^2 - v^2) \qquad (11)$$

If T_o is taken at the state of rest ($v_o = 0$), equation (10) becomes:

$$C_p(T_o - T) = \frac{1}{2Jg}v^2$$

Using C_p in the units of foot-pounds/degree Rankine:

$$C_p(T_o - T) = \frac{1}{2g}v^2 \text{ or } v^2 = 2gC_p(T_o - T) \qquad (12)$$

The energy equation in the case of frictionless water flow states that the sum of the potential energy and the kinetic energy of a water particle is constant.

Consider a flow filament (Fig. 1) which passes through the point y_o, z_o of the initial cross section $x = 0$. Along this filament, between the pressure P and the velocity v, the energy equation is:

$$P + \tfrac{1}{2}\rho v^2 + \rho gz = \text{Constant} = P_o + \tfrac{1}{2}\rho v_o^2 + \rho gz_o \qquad (13)$$

On the free surface of the water P is constant and equal to the atmospheric pressure, Pa. In what follows, we may, without error, set this to zero since only differences in pressure are of physical significance in the case of incompressible flows. If the water flows from an infinitely wide basin then $v_o = 0$. The curvature of the free surface is also zero at this point. It is logical to choose this point as the reference point x_o, y_o, z_o. The corresponding water depth is denoted by h_o. For the above reference point, the Bernoulli equation is:

$$P + \tfrac{1}{2}\rho v^2 + \rho gz = P_o + \rho gz_o$$

or

$$v^2 = 2g(z_o - z) - 2(P_o - P)/\rho \qquad (14)$$

It is reasonable to assume that the vertical acceleration of the water is negligible compared with the acceleration of gravity. Under this assumption the static pressure at a point in the field of flow varies linearly with the vertical distance from that point to the free surface:

$$P_o = \rho g(h_o - z_o) \qquad (15)$$

and

$$P = \rho g(h - z) \qquad (16)$$

Substituting (15) and (16) in (14) gives:

$$v^2 = 2g(h_o - h) = 2g\Delta h \qquad (17)$$

The above energy equation is valid for the flow filament passing through y_o and z_o at $x = 0$. Since, at $x = 0$, all the filaments which lie one above the other have the same h_o and v_o (zero), and since equation (17) does not contain z, the velocity v at x and y is constant over the entire depth and is equal to the difference in height between the total head (ho) and the free level (h), (Δh), at most can equal h_o. The maximum velocity, therefore is

$$v_{max} = \sqrt{2gh_o}$$

If we write equation (17) in dimensionless form:

$$\left(\frac{v}{v_{max}}\right)^2 = \frac{\Delta h}{h_o} = 1 - \frac{h}{h_o} \qquad (18)$$

From equation (12) it is obvious that the maximum velocity in a gas is:

$$v_{max} = \sqrt{2gC_pT_o}$$

and

$$\left(\frac{v}{v_{max}}\right)^2 = \frac{2gC_p\Delta T}{2gC_pT_o} = \frac{\Delta T}{T_o} = 1 - \frac{T}{T_o} \qquad (19)$$

From equations (18) and (19) it may be seen that the ratio of the velocity to the maximum velocity for the water and the gas flows becomes equal if

$$1 - \frac{h}{h_o} = 1 - \frac{T}{T_o}$$

or

$$\frac{T}{T_o} = \frac{h}{h_o} \qquad (20)$$

Equation (20) shows that, with respect to the velocity, there exists an analogy between the two flows if the depth ratios are compared with absolute gas temperature ratios.

By comparing the equation of continuity for the water flow with a free surface to that of a gas, it is possible to obtain another analogy.

Consider at x,y, a small fluid prism with the dimensions dx, dy, and h (Fig. 2). Let a, b, and c represent the components of the velocity in the direction of the x, y, and z axes respectively.

If the assumption is made that the vertical acceleration of the water is negligible in comparison to the acceleration of gravity, equation (16) can be used in differential form as:

$$\frac{\partial P}{\partial x} = \rho g \frac{\partial h}{\partial x}$$

and

$$\frac{\partial P}{\partial y} = \rho g \frac{\partial h}{\partial y}$$

The right sides of the above equations are independent of z, which means that the horizontal accelerations of all points along a vertical are also independent of z. The horizontal components, a and b, are then constant over the depth h.

The continuity equation for this type of water flow states that the rate of mass flow into the prism is equal to the rate of flow out of the prism. Since the density of the water is constant, the inflowing volume per unit time (dQ_{In}) must equal the outflowing volume (dQ_{Out}).

$$dQ_{In} = ahdy + bhdx$$

and

$$dQ_{Out} = (a + \frac{\partial a}{\partial x}dx)(h + \frac{\partial h}{\partial x}dx)dy + (b + \frac{\partial b}{\partial y}dy)(h + \frac{\partial h}{\partial y}dy)dx$$

By expanding and neglecting infinitely small magnitudes of higher order, we have:

$$\frac{\partial (ha)}{\partial x} dxdy + \frac{\partial (hb)}{\partial y} dxdy = 0$$

and dividing by dxdy:

$$\frac{\partial (ha)}{\partial x} + \frac{\partial (hb)}{\partial y} = 0 \qquad (21)$$

Equation (21) is the continuity equation for stationary water flow.

The continuity equation for a two dimensional compressible gas flow is:

$$\frac{\partial(\rho a)}{\partial x} + \frac{\partial(\rho b)}{\partial y} = 0 \qquad (22)$$

Equations (21) and (22) obviously have the same form. From these equations it is possible to derive a further condition for the analogy of the two flows, namely, that the density of the gas flow corresponds to the depth, h, of the water. Expressing this analogy as a dimensionless ratio:

$$\frac{\rho}{\rho_o} = \frac{h}{h_o} \qquad (23)$$

It is now possible to investigate the physical nature of this gas which we are comparing with the flow of water with a free surface. The adiabatic equation (8) states that:

$$\frac{\rho}{\rho_o} = \left(\frac{T}{T_o}\right)^{\frac{1}{\gamma-1}}$$

From (20) and (23) we have:

$$\frac{T}{T_o} = \frac{h}{h_o} \quad \text{and} \quad \frac{\rho}{\rho_o} = \frac{H}{h_o}$$

By substituting these values in equation (8), we have the equation:

$$\frac{H}{h_o} = \left(\frac{h}{h_o}\right)^{\frac{1}{\gamma-1}}$$

which obviously is satisfied only if

$$\underline{\gamma = 2.0}$$

Thus it is shown that the flow of the water is quantitatively comparable with the flow of a gas having a ratio $\gamma = \frac{C_p}{C_v}$ equal to 2.0

Another analogy, probably the most important from an experimental point of view, is obtained from the gas equation:

$$P = \rho RT$$

or

$$\frac{P}{P_o} = \frac{\rho}{\rho_o} \frac{T}{T_o}$$

By substituting the values of $\frac{\rho}{\rho_o}$ and $\frac{T}{T_o}$ in terms of $\frac{h}{h_o}$ we have:

$$\frac{P}{P_o} = \left(\frac{h}{h_o}\right)^2 \qquad (24)$$

Equation (24) can also be derived by using either of the adiabatic equations (6) or (9) and $\gamma = 2.0$.

For a compressible gas, the velocity of propagation of a sound wave $v_s^2 = \sqrt{\gamma g R T}$.[1] The velocity of propagation of a surface wave in shallow water is $v_s^2 = \sqrt{gh}$.[2] This velocity is called the "critical velocity".

In a gas expanding through a nozzle there is a critical pressure ratio at which sonic velocity occurs at the throat. In the case of air with a $\gamma = 1.385$, the critical pressure ratio is $\frac{P_o}{P_T} = 1.852$. If the ratio of the pressure at the nozzle entrance to the throat pressure $\left(\frac{P_o}{P_T}\right)$ is less than this value, sonic velocity cannot occur in the nozzle throat. An analogous condition occurs in the water flow.

The critical velocity of water is $\sqrt{gh}$. From the energy equation (17) we have:

---

1. Neil P. Bailey, "The Thermodynamics of Air at High Velocities."
2. Earnst Preiswerk, "Application of the Methods of Gas Dynamics to Water Flows with Free Surface", Part I, NACA TM 934, p. 6, 1940.

$$v^2 = 2g(h_o - h)$$

By substituting $v_w^* = \sqrt{gh}$, equation (17) becomes

$$gh = 2gh_o - 2gh$$

or

$$\frac{h}{h_o} = \frac{2}{3}$$

Then at any point where the water depth is two thirds of the total head, the water is flowing at the critical velocity.

In air, if the Mach number ($M = \frac{v}{v_w}$) is less than one, the flow is said to be "subsonic" and if M is greater than one, the flow is "supersonic". In water, if $\frac{v}{v_w}$ is less than one, the flow is known as "streaming flow" and if $\frac{v}{v_w}$ is greater than one, the flow is "shooting flow".

If air is flowing at supersonic velocity, a discontinuity may occur in which the velocity suddenly decreases to a subsonic value which satisfies the conditions of flow.[3] This discontinuity is called a "plane compression shock" and theoretically takes place in a very short distance. Just as the velocity suddenly decreases through a plane shock, the pressure suddenly increases. When supersonic gas flow is forced to change its flow direction due to an obstruction, an "angle shock" will occur.[4] It is known that an analogous discontinuity, called the "hydraulic jump", may occur in shooting water flow. As in a gas, two cases of the jump are possible: (a) In the right jump, shooting water is con-

---

3. Neil P. Bailey, "Abrupt Energy Transformations in Flowing Gases", Appendix B, p. 2.
4. Ibid, p. 3.

verted into streaming flow and (b) in the slant or oblique jump, the flow may or may not go to streaming after the jump, depending on the $\frac{V}{V_w^*}$ of the water.

A summary of the flow analogy is as follows:

	TWO DIMENSIONAL GAS FLOW	LIQUID FLOW WITH FREE SURF IN GRAVITY FIELD
Nature of flow medium	Hypothetical gas with $\gamma = 2.0$	Incompressible fluid (wate
Side boundaries	Geometrically similar	Side boundary vertical Bottom horizontal
Analogous magnitudes	Velocity $\frac{v}{v_{max}}, \frac{v}{v_g^*}$	Velocity $\frac{v}{v_{max}}, \frac{v}{v_w^*}$
	Temperature ratio, $\frac{T}{T_o}$	Depth ratio, $\frac{h}{h_o}$
	Density ratio, $\frac{\rho}{\rho_o}$	Depth ratio, $\frac{h}{h_o}$
	Pressure ratio, $\frac{p}{p_o}$	Square of depth ratio, $(\frac{h}{h_o})$
	Sound velocity, v_g^*	Wave velocity, v_w^*
	Mach Number, $\frac{v}{v_g^*}$	Mach number, $\frac{v}{v_w^*}$
	Subsonic flow	Streaming flow
	Supersonic flow	Shooting flow
	Compression shock (plane and angle)	Hydraulic jump (normal and slant)

Thus far we have shown the analogy that can be made between water and a gas having a γ of 2.0. The analogy between the compression shock and the hydraulic jump, however, does not strictly hold. The energy equation (17) between the velocity and the depth for water flow is:

$$v^2 = 2g(h_o - h)$$

where the total head, (h_o), is constant. In the case of the hydraulic jump a portion of the kinetic energy of the water is converted into heat. For this reason the total head after the jump, (h_j), is smaller than the total head before the jump, (h_o). After the jump the energy equation is:

$$v^2 = 2g(h_j - h)$$

The energy loss during the jump bears a simple relation to the intensity of the jump. In the flow over a horizontal bottom the potential energy is a minimum if the water depth, h, is zero. For a mass of water, m, at a depth, h, the potential energy is $P = mgh/2$.

Since the kinetic energy at points of rest is equal to zero, the energy loss, (Δe), which occurs in the hydraulic jump may be computed as the difference of the potential energy at a point of zero velocity before and after the jump, or

$$\Delta e = mg\left(\frac{h_o}{2} - \frac{h_j}{2}\right) \qquad (25)$$

By dividing this energy loss by the energy before the jump, $e = mg\frac{h_o}{2}$, the relative energy loss is obtained as:

$$E = \frac{\Delta e}{e} = 1 - h_j/h_o \qquad (26)$$

This is the relative amount of energy which has been converted into heat and is lost energy insofar as water is concerned.

In a gas, the heat generated by a shock is not lost, but is merely converted into thermal energy, and the total temperature, consequently the total energy, is the same before and after the shock. Since the comparable water magnitude to the gas temperature is the depth, the analogy is not strictly true after a hydraulic jump. The energy loss in water[5] is extremely small over a large region of jump intensity, the relative loss being less than one percent for $\frac{V}{V_w}$ up to 3.0. As a result of this small shock energy loss, the analogy of the two types of flow is still valid as a very close approximation within the range of Mach numbers currently employed.

---

5. Preissmerk, Op. cit, Part II, p. 21-22

PART II

CONSTRUCTION OF THE R.P.I. WATER TABLE

The essential element of a water table is a horizontal surface with vertical sides over which a shallow stream of water flows. The necessary adjuncts to the surface are a framework to support it, the tanks, pump, and piping to supply the flowing water, and the necessary measuring instruments. The following description of the water table constructed in the Mechanical Engineering Laboratory at the Rensselaer Polytechnic Institute will serve to illustrate one method of fabrication.

The surface is a sheet of plate glass, ¼" x 48" x 60". Glass was selected for two reasons. First, glass is one of the most frictionless surfaces obtainable sufficiently rigid to maintain a horizontal plane. Second, the use of glass makes possible the taking of photographs of the flow either from above or underneath the surface of the table, illumination being supplied on the side opposite to the camera.

The frame is constructed of white pine. The table box is constructed of 2" x 6" plank, the legs of 4" x 4" timbers, and the crossbars and leg braces of 2" x 4" stock. An isometric drawing of the frame is shown in Fig. 3, and actual dimensions can be found in Fig. 4. All joints are mortised and secured by bolts. To provide for leveling the table, the bottom of each leg is fitted with a ¼" steel plate into which is threaded a ½" steel bolt.

The glass is supported on the sides by 1" x 2" strips of wood screwed to the frame and the forward and after ends rest in grooves cut in the 2" x 4" crossbars. Details of the support arrangement are shown in Fig. 7. Two 1" angle irons, surfaced with masonite, placed one-third the length of the glass from each end, supply support across the table. The glass is held firmly in place by 1" x 2" wood strips running the length of the table. These strips are covered with copper flashing in order to provide smooth vertical walls and to prevent the possibility of warping due to water-to-wood contact. To insure watertightness and avoid a metal-to-glass contact, a strip of ¼" sponge rubber is secured between the copper and the glass.

The tanks are constructed of 18-gauge rolled sheet steel. Dimensions of the forward tank are shown in Fig. 5. This tank has a capacity, up to the lip, of about five cubic feet. The forward tank is bolted to the frame on three sides. The four-inch lip rests upon the forward 2" x 4" crossbar and projects over the forward edge of the glass. The lip is prevented from direct contact with the glass by a strip of ¼" sponge rubber. A three-inch flange with a standard 1½" pipe thread is brased to the bottom of the tank to accommodate the supply pipeline.

Dimensions of the after tank are shown in Fig. 6. It has a capacity, up to the lip, of about 3.3 cubic feet. The after tank is bolted to the after end of the frame and the one-inch lip rests in a groove cut in the after 2" x 4"

crossbar. A strip of copper flashing runs from the after edge of the glass, over the tanklip, and into the tank. This provides a smooth surface for the water flow and prevents water-to-wood contact. Three four-inch flanges with standard two-inch pipe thread are brased to the bottom of the tank to accommodate the discharge pipelines.

The water for this table is self-contained and recirculating. For this purpose there is an 80-gallon capacity sump tank at the after end of the table. The piping and connections between the pump, two table tanks, and sump tank are shown in Fig. 4. Since the pump is an alternating current electric-driven constant speed centrifugal type, a controlling valve on the discharge side of the pump and a water by-pass line are used to throttle and divert the flow. All piping is two-inch steel except for the by-pass line and short section leading into the forward tank, which are 1½" steel. Valves are located in the three discharge lines from the after tank to regulate back pressure on the table surface.

To measure water flow, there is a flat plate orifice, 1.25" in diameter, in the 1½" line leading to the forward tank. Pressure taps, located in accordance with the ASME research publication on fluid meters[6], are connected by rubber tubing to a U-tube water-filled manometer. The orifice and manometer were calibrated by weighing the

---

6. "Fluid Meters, Their Theory and Application," Part I, ASME Research Publication, 1931.

amount of water flowing in a measured interval of time. A calibration curve is shown in Fig. 9.

To measure depth on the water table surface, a hook gauge, capable of measuring to 1/1000 foot is used. The hook was replaced by a straight pointed rod for greater convenience and accuracy. The gauge is mounted on a wooden block which slides freely along a 2" x 2" wooden stringer. The stringer rests on the table frame. Depth is measured by taking the difference of a reading at the glass and one at the water surface.

A wire basket filled with small rocks is used to smooth out the water flow. This basket is fabricated of two strips of $\frac{1}{2}$" wire mesh which are three inches apart. The basket rests in the center of the forward tank and runs the width of the tank. It also serves the purpose of a water filter. Two weirs are provided to supply the necessary total head. They are fabricated of 14 gauge sheet brass, rolled and bent to the desired shape. The underneath side of each weir is fitted with three equally spaced wooden blocks into each of which is secured a $\frac{1}{4}$" bolt. The wooden blocks are held in place by small brass machine bolts which are countersunk into the top of the weir. The bolt heads are covered with solder which was smoothed to conform to the shape of the surface of the weir. The securing bolts project through holes in the lip of the forward tank and crossbar and are secured by nuts bearing against the underside of the crossbar. Watertightness is maintained by using caulking compound between the weir and the table sides and

tank. Details are shown in Fig. 7.

The wooden models used thus far in conjunction with experiments on the table were fabricated of white pine and finished with spar varnish, sanded to a fine polish.

To minimize surface tension, a wetting agent is used in the water.

Fig. 10 is a photograph of the completed table in which the frame, pump, piping, valves, manometer, and depth gauge are visible.

Fig. 11 is a photograph of the table top looking forward, in which the glass, weir, and rock filter are visible. A typical experimental set-up is shown in place on the glass.

In the course of construction two major difficulties were encountered, mounting the glass and obtaining laminar flow.

The original intention was to use ½" plate glass both for rigidity and strength. This glass could not be obtained within the time available. After investigation of strength and rigidity properties, ¼" plate glass was determined to be satisfactory and was installed. This glass was supported only on the four sides. About one month after installation, this glass fractured. Apparently, the glass had sagged slightly in the center and the stress set up, in time, resulted in fracture. A second ¼" plate glass was installed and the two angle iron braces were added as additional support. After about three weeks, a small fracture was experienced at the after corner of the table. The cause of

this second break is not definitely known. No impact spot is discernible and the glass is perfectly level. This break does not affect the operation of the table. A sheet of ½" plate glass has been ordered and will be installed as soon as delivered.

The Reynolds number of the flow on the table is very near the critical. In order to obtain laminar flow, the water must proceed from its entrance into the forward tank, through the rock filter, over the weir and on to the table with gradual turns. The weir surface must be extremely smooth since any protuberance will set up a disturbance and force the water into turbulent flow. The first weir used was constructed of wood. A really smooth surface could not be obtained on the wood available, and this was discarded in favor of the weir constructed of brass. Laminar flow is now obtained throughout the practical range of flow velocities.

PART III

APPLICATIONS OF THE WATER TABLE

The applications of the water table in connection with the study of air flow are many in number. The water table may be used to study any type of two-dimensional air flow which does not involve a change in the total energy. Some of the more important applications, in the opinoin of the writers, are as follows:

(1) the investigation of the flow of supersonic air in and around airfoils, inlets, nozzles, and diffusers. Models must be designed and fabricated for air flow with a $\gamma = 2.0$.

(2) confirmation of the validity of assumptions made in the development of air flow theory. Using $\gamma = 2.0$ in the equations, the theory can be checked with experimental results obtained from the water table. The water table offers an excellent medium for studying the little known transsonic region.

(3) as a laboratory apparatus for demonstrating the accepted theory of various types of gas flow.

One example of the applications of the water table is demonstrated in the case of flow of supersonic air around a simple wedge. The purpose of the experiment was to check the water analogy with the existing theory on angle shocks.[7]

---

7. Bailey, Op. cit, p. 4.

A sketch of the wedge used in the experiment is shown in Fig. 8. Experimental data can be found in Table I. Table II contains the results calculated from the experimental data. Table III contains the results calculated for air with a $\gamma = 2.0$. Sample calculations can be found in Appendix A. A comparison of Tables II and III, shows the correlation between the water table analogy and air flow is within the limits of experimental accuracy.

SUMMARY

The theory of the analogy of two dimensional air flow to the flow of water with a free surface has been presented.

The details of construction of the water table, which utilizes the water analogy in the study of air flow, has been described.

The operation and an application of the water table have been demonstrated.

The water table could be employed to a decided advantage by the organizations which use the few supersonic wind tunnels in existance in this country to study the flow of high velocity air. Much of the work done at present in the wind tunnels could be accomplished on a water table with the resultant considerable saving in time and expense.

The emphasis in this work has been on supersonic air flow, however, the water table can be used for subsonic air flow investigations. It is a fine laboratory apparatus for demonstrating hydraulic and air flow theory visually.

The operation of the present water table would be enhanced with the use of a depth gauge capable of measuring to 1/1000 inch. A further refinement in control of water flow is necessary. It is suggested that the present pump and motor be replaced by a controllable direct current electric drive variable speed centrifugal pump. It is also suggested that inorder to accurately measure shock angles on photographs, a parallel light system be constructed.

BIBLIOGRAPHY

1. Bailey, Neil P. - "The Thermodynamics of Air at High Velocities", Volume II, No. 3, Journal of the Aeronautical Sciences.
2. Bailey, Neil P. - "Abrupt Energy Transformation in Flowing Gases."
3. Bakhmetev, B. A. - "Hydraulics of Open Channels." The McGraw-Hill Book Company, New York, 1934.
4. "Fluid Meter, Their Theory and Application", Part I. Report of Association of Mechanical Engineers Special Committee on Fluid Meters. ASME Research Publication, New York, 1931.
5. Preiswerk, Ernst - "Application of the Methods of Gas Dynamics to Water Flows with Free Surface." Technical Memorandums Numbers 934 and 935, National Advisory Committee for Aeronautics.

APPENDIX A

SAMPLE CALCULATIONS

Run I

A = cross sectional area of water flow, equal to hw, ft.²

M_w = mach number of water flow, v_w/v_w^*

v_w = water velocity, fps

v_w^* = velocity of propogation of a surface wave, fps

w = width of water flow, ft.

θ = shock angle, deg.

Water Flow

$v_w = Q/A = Q/hw = 0.865$ ft/sec

$v_w^* = \sqrt{gh} = \sqrt{32.2 \times .006} = 0.440$ ft/sec

$M_w = 0.865/0.440 = 1.965$

$h_o/h_1 = \left[1 - \frac{\gamma-1}{2} M_1^2\right]^{\frac{\gamma}{2(\gamma-1)}} = \left[1 - 0.5 \times 3.86\right] = 2.025$

$h_2/h_1 = .810/.006 = 1.667$

$P_2/P_1 = (h_2/h_1)^2 = (1.667)^2 = 2.775$

$h_o/h_2 = h_o/h_1 \times h_1/h_2 = 2.025/1.667 = 1.755$

$M_2 = \sqrt{2\left(\frac{h_o}{h_2} - 1\right)} = \sqrt{2(.753)} = 1.230$

Air Flow ($\gamma = 2.0$)

$$P_2/P_1 = \frac{2\gamma M_1^2 \sin^2\theta}{\gamma-1} - \frac{\gamma-1}{\gamma+1} = \frac{4 \times 3.86 \times .868}{3} - \frac{1}{3} = 3.01$$

$$M_2 = \frac{1}{\sqrt{\left[1 - \frac{\frac{\gamma-1}{2} M_1^2}{M_1^2 \cos^2\theta}\right] \cos^2(\theta - \alpha) - \left(\frac{\gamma-1}{2}\right)}}$$

$$= \frac{1}{\sqrt{\frac{(1 - 0.5 \times 3.86)\ 0.868}{3.86 \times 0.345} - \frac{1}{2}}} = 1.057$$

Table I

Fifteen Degree Wedge

Experimental Measurements

Run No.	Manometer	Q	h_1	h_2	θ
	inches H_2O	ft^3/sec	ft	ft	deg.
1	5.1	.0201	.006	.010	54
2	7.6	.0357	.006	.012	38
3	15.4	.0550	.006	.017	18

Table II

Fifteen Degree Wedge

Calculated Values

Run No.	V_o	V_n	M_1	h_o/h_1	h_2/h_1	P_2/P_1	h_o/h_2	M_2
	fps	fps	-	-	-	-	-	-
1	0.685	0.440	1.562	2.815	1.667	2.775	1.753	1.430
2	1.38[illegible]	0.440	2.815	5.250	2.000	4.000	2.625	1.414
3	1.380	0.440	3.400	20.55	1.830	8.000	7.280	1.540

Table III

Fifteen Degree Wedge

Calculated Values for Air with γ = 1.4

Run No.	M_1	P_2/P_1	M_2
1	1.962	3.08	1.697
2	2.915	9.98	1.700
3	5.400	8.18	2.210

FIGURE 1

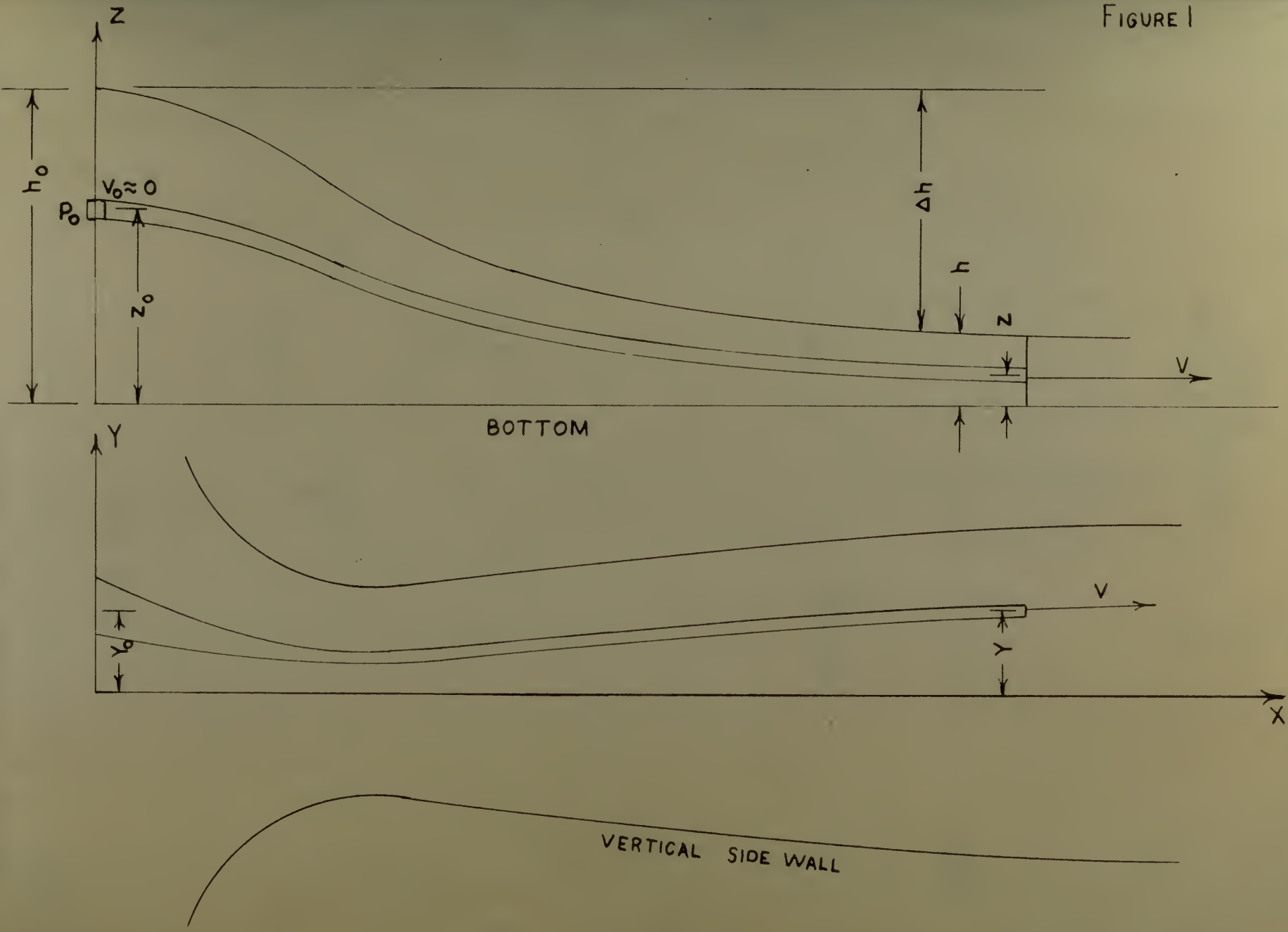

ENERGY EQUATION NOTATION

R.A THOMPSON

FIGURE 2

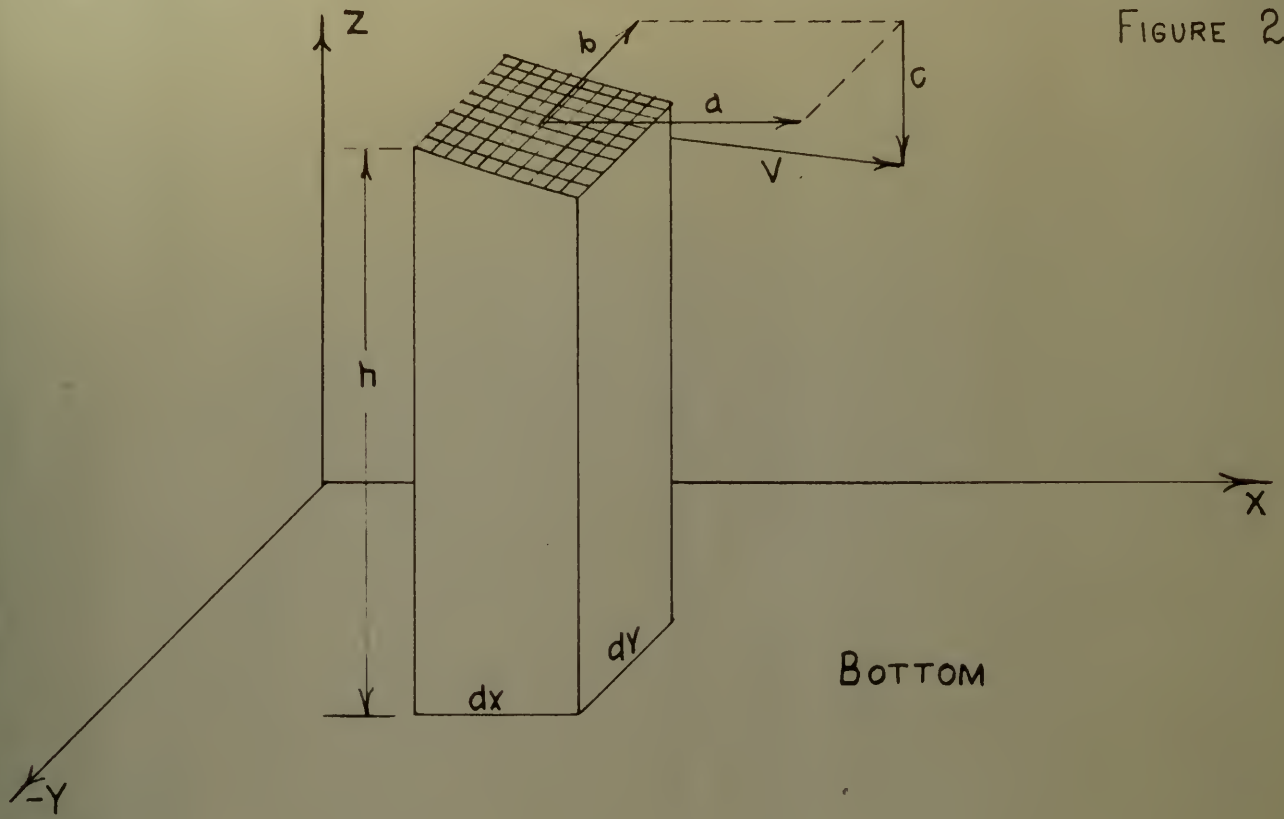

BOTTOM

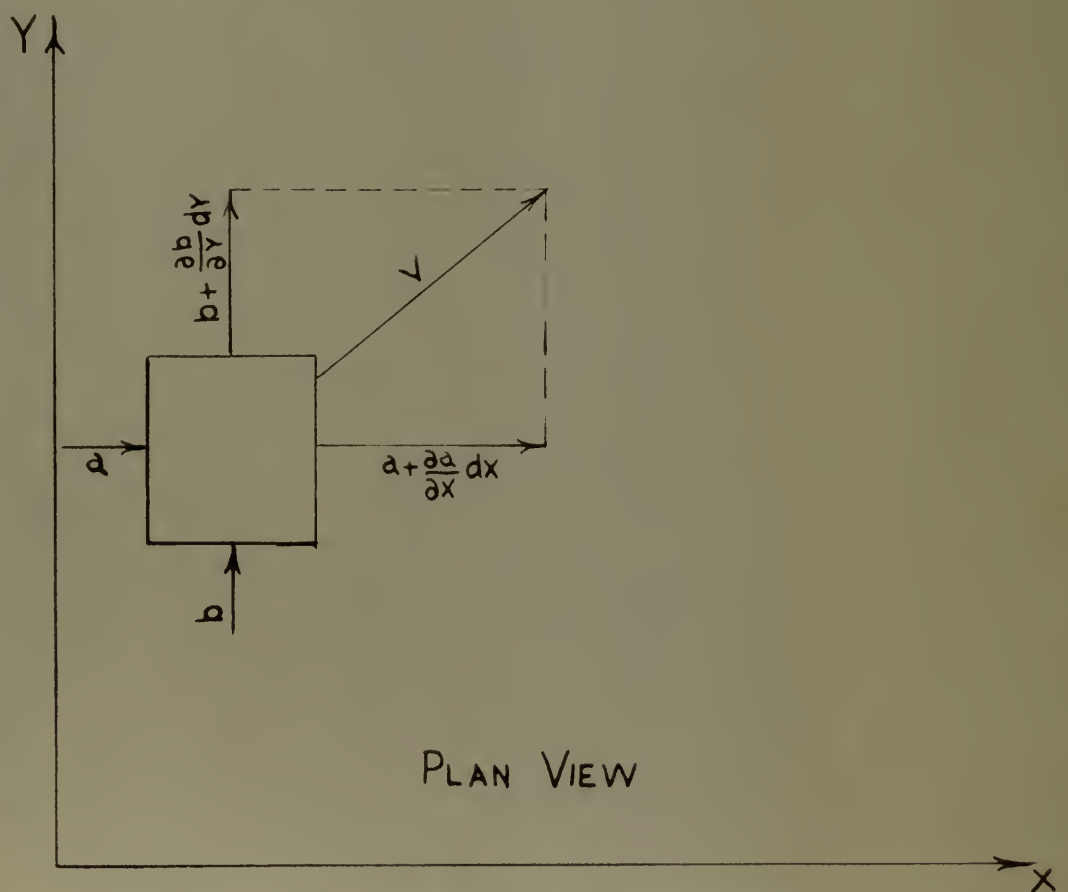

PLAN VIEW

NOTATION FOR CONTINUITY EQUATION

R.A. THOMPSON

37

FIGURE 3

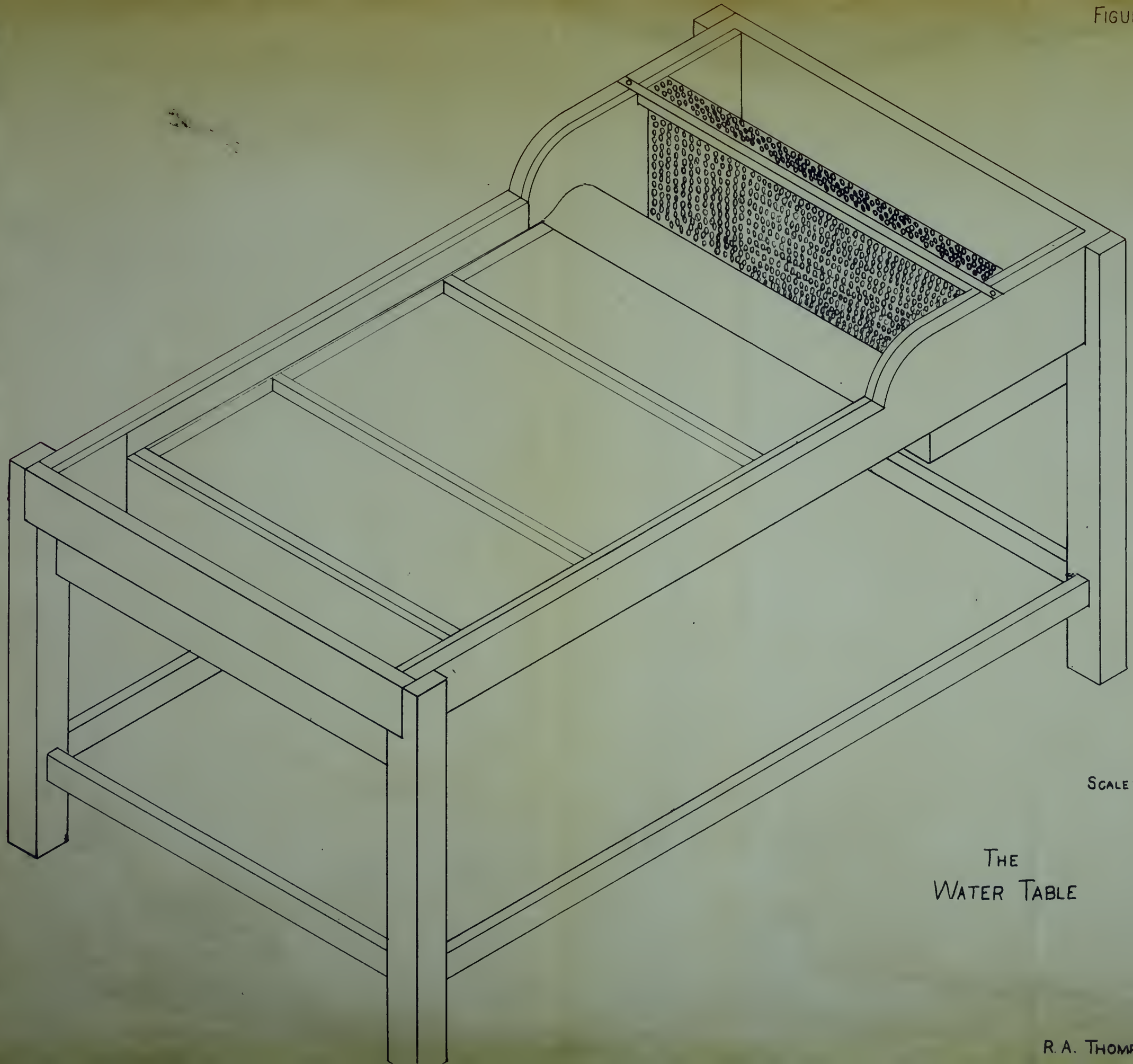

SCALE: 1½" = 1'

THE WATER TABLE

R. A. THOMPSON

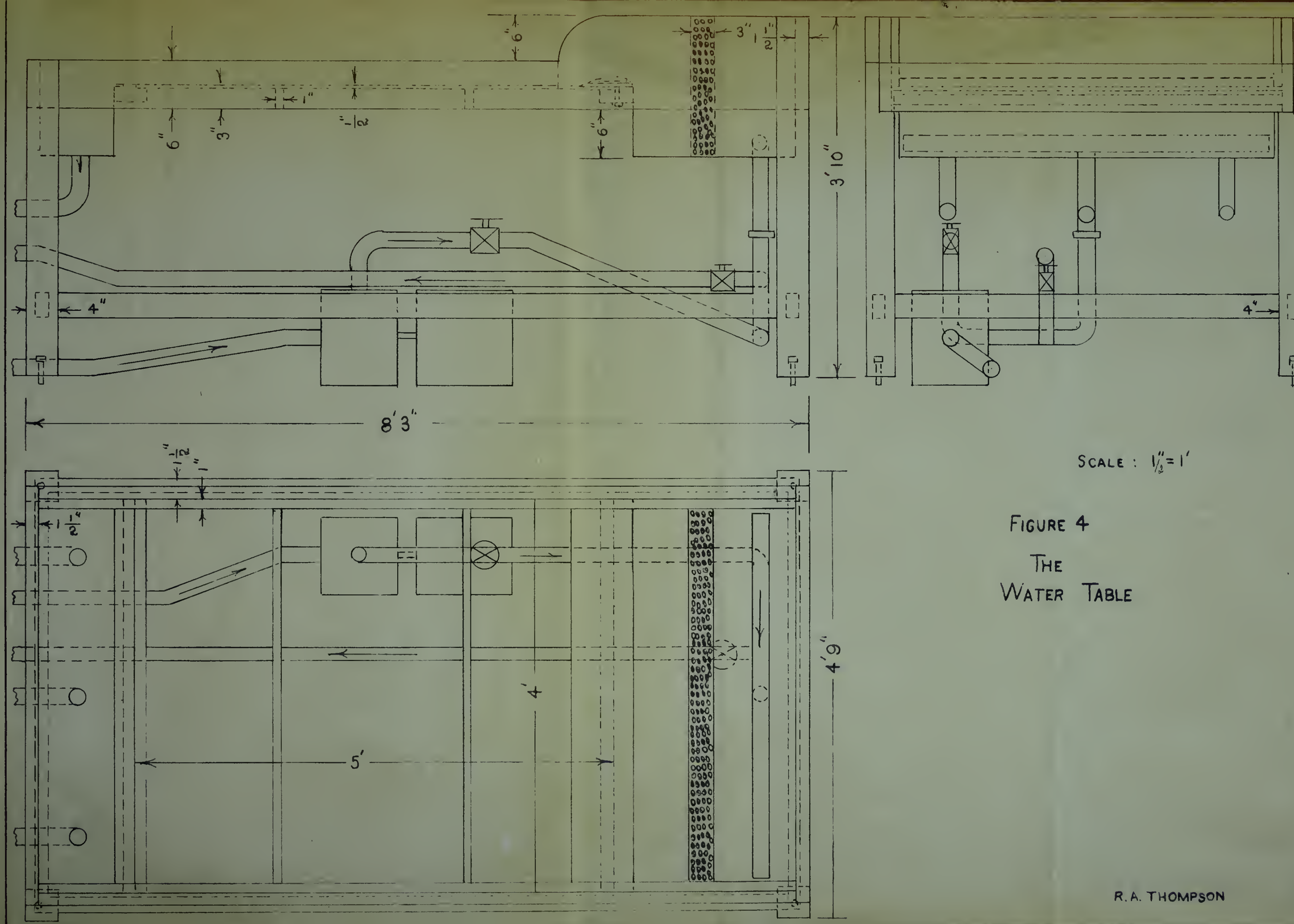

SCALE : 1½" = 1'

FIGURE 4

THE
WATER TABLE

R. A. THOMPSON

FIGURE 5

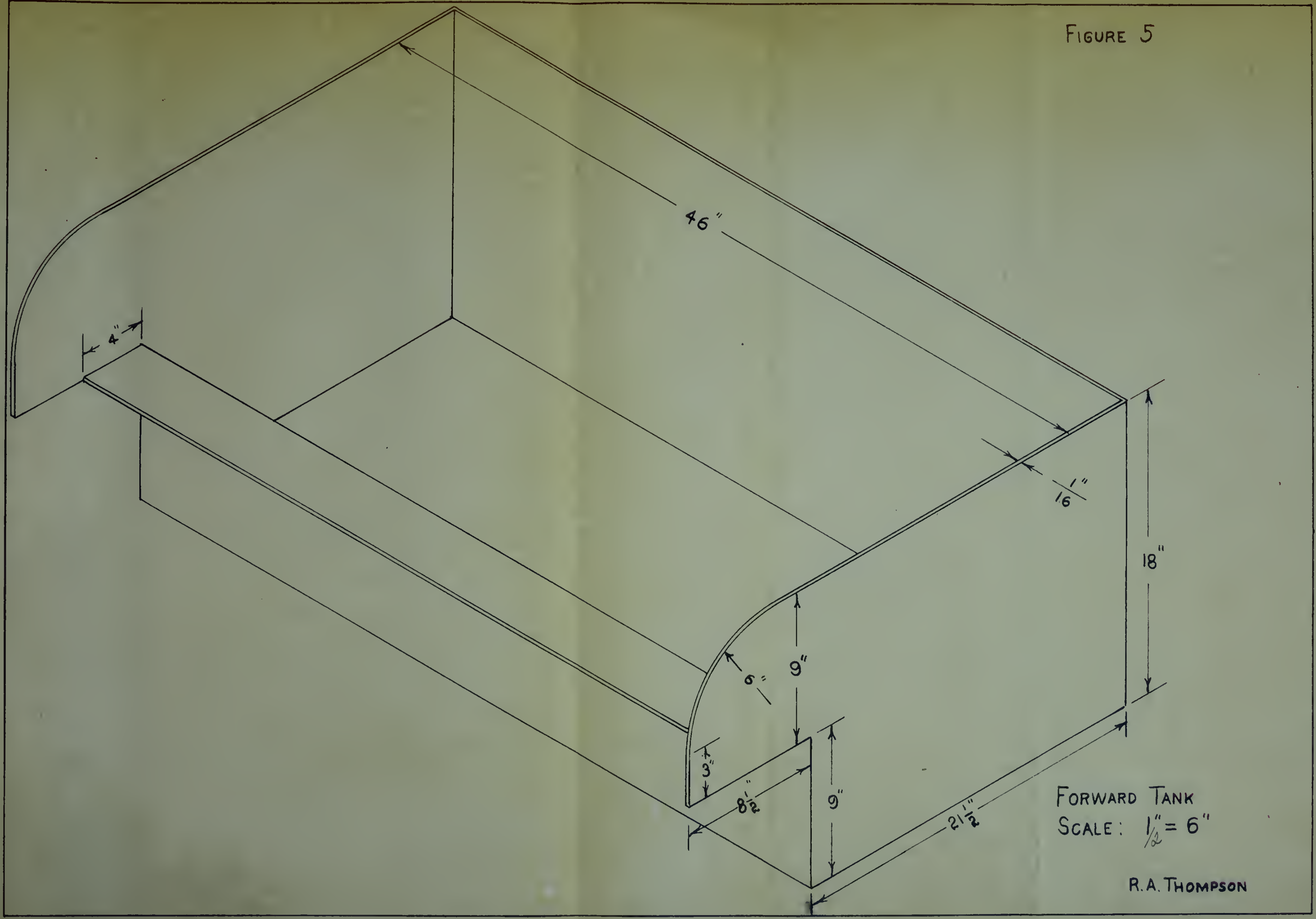

FORWARD TANK
SCALE: 1/2" = 6"

R.A. THOMPSON

FIGURE 6

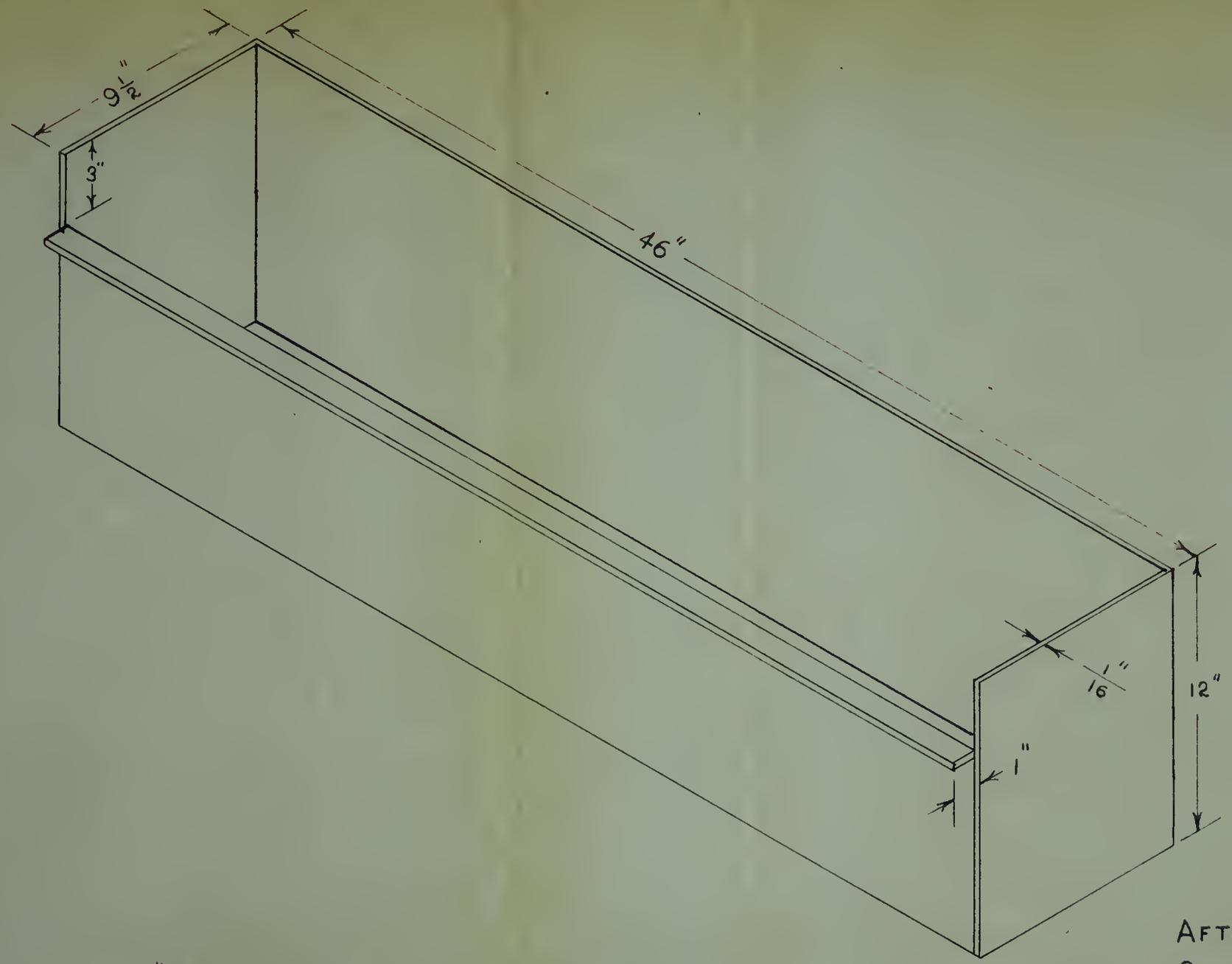

AFTER TANK
SCALE: 1½" = 6"

R.A. THOMPSON

FIGURE 7

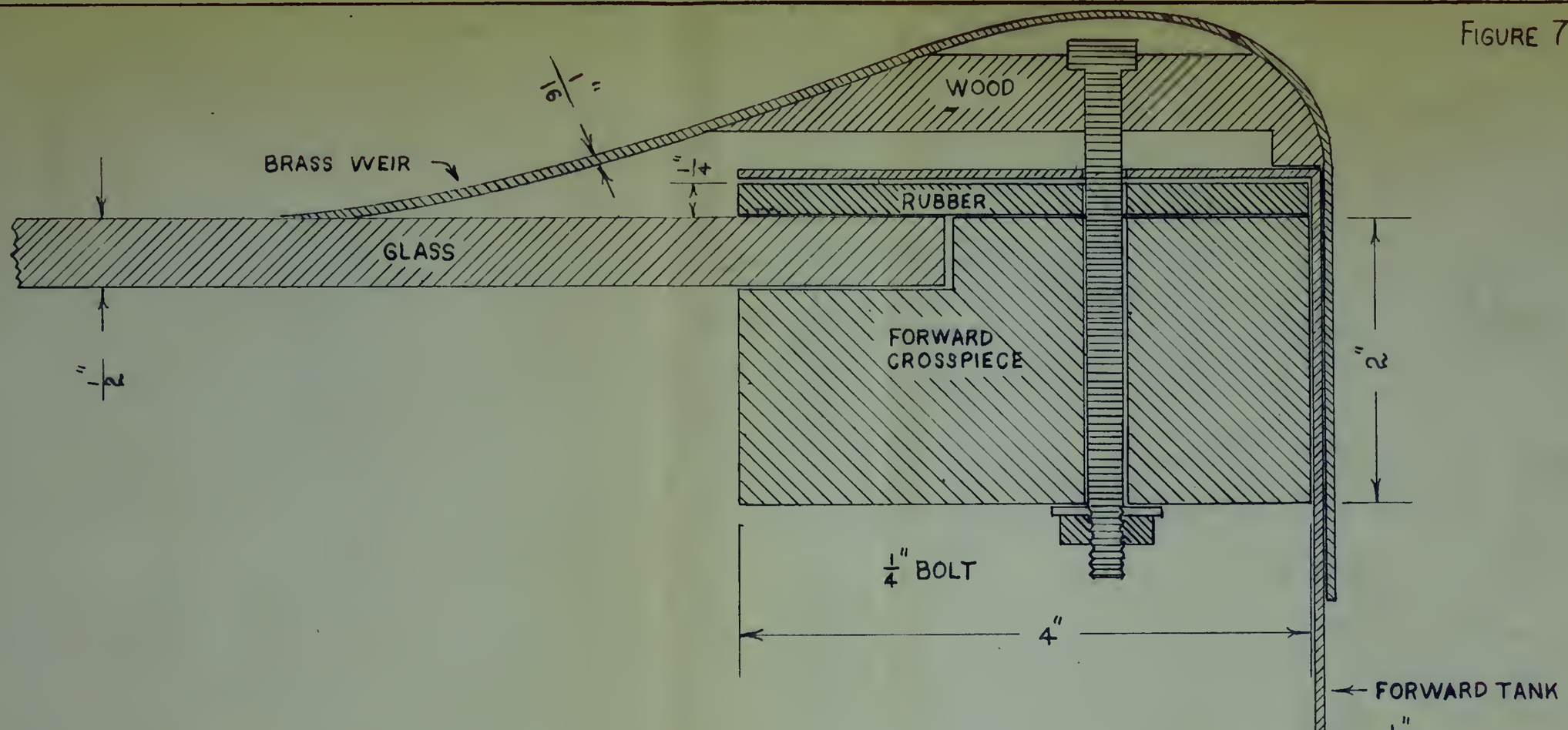

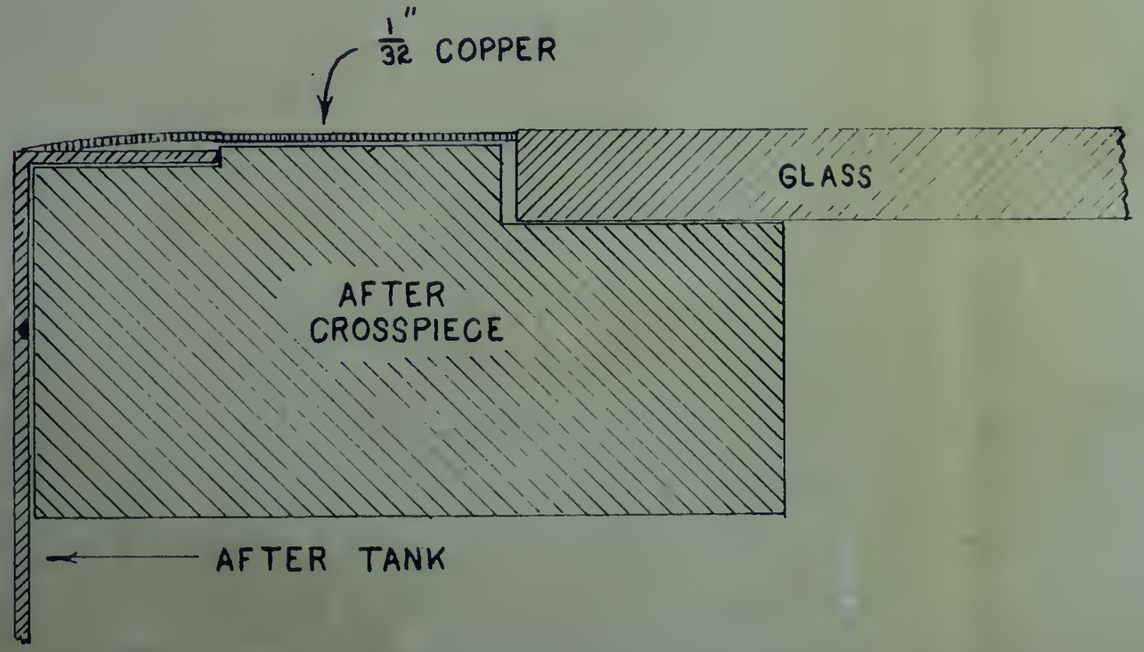

ASSEMBLY DETAILS
OF
FORWARD AND AFTER
CROSSPIECES
SCALE: 1/2 FULL

R.A. THOMPSON

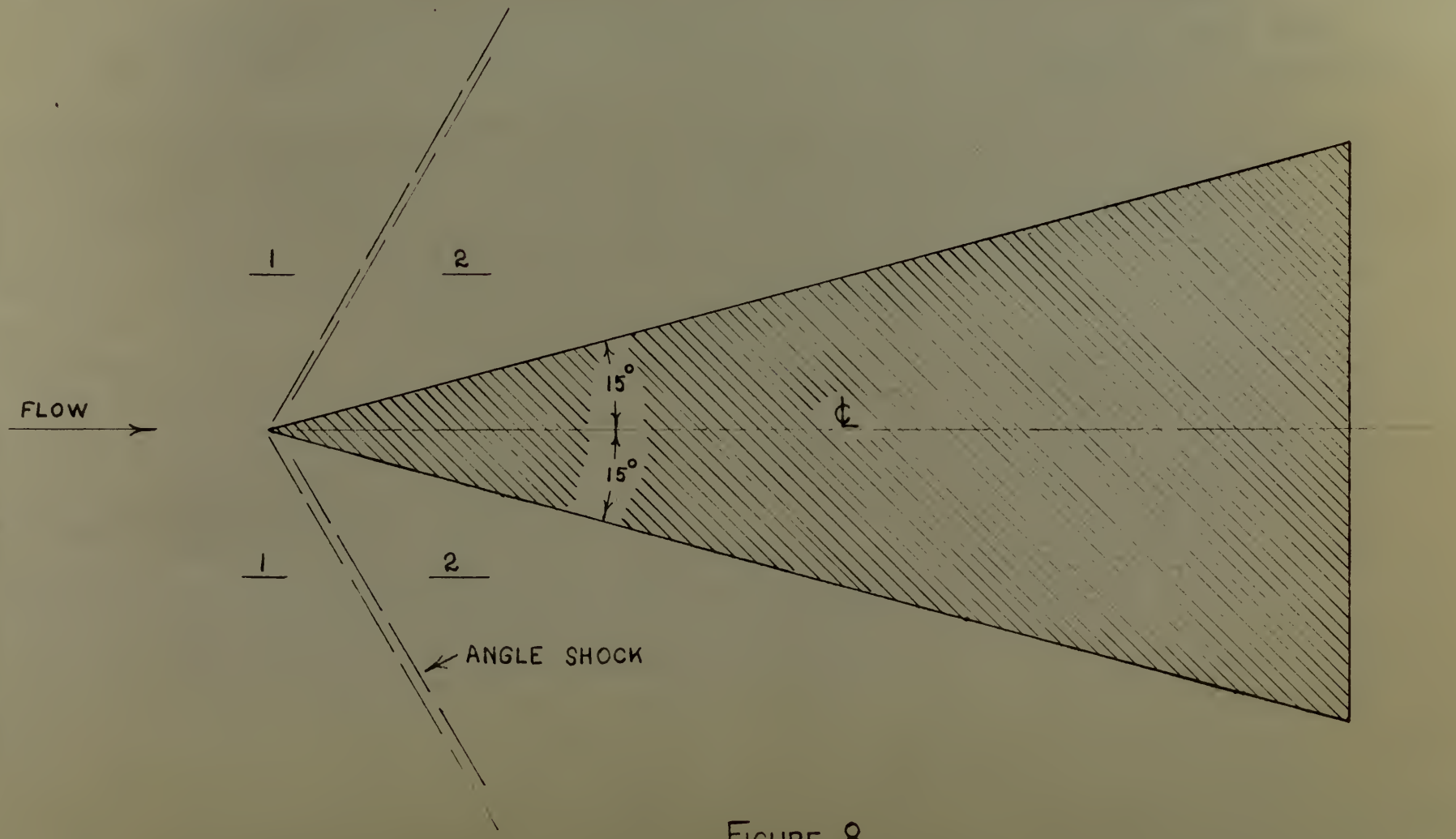

FIGURE 8
WEDGE
SCALE: FULL

R.A. THOMPSON

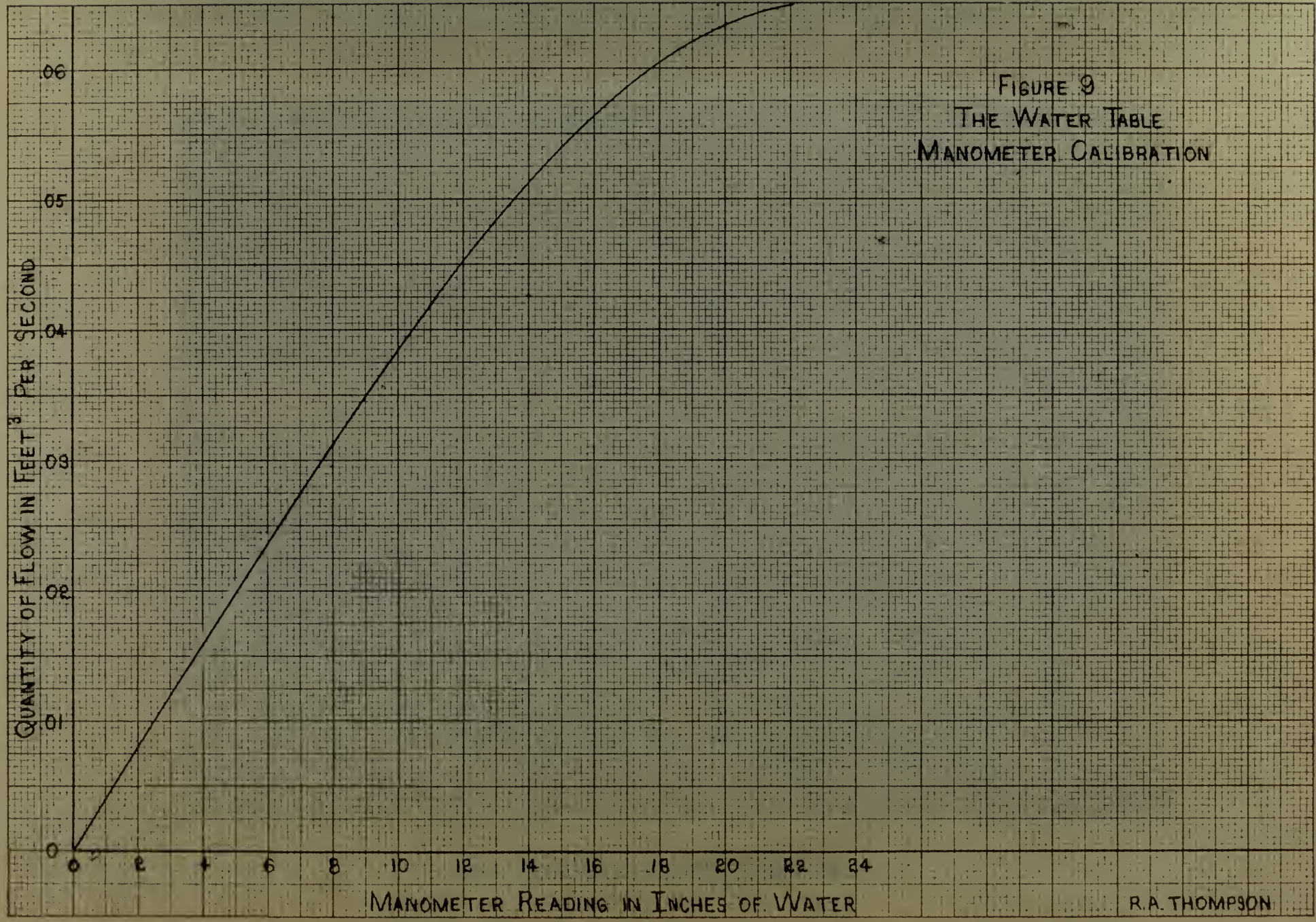

FIGURE 9
THE WATER TABLE
MANOMETER CALIBRATION

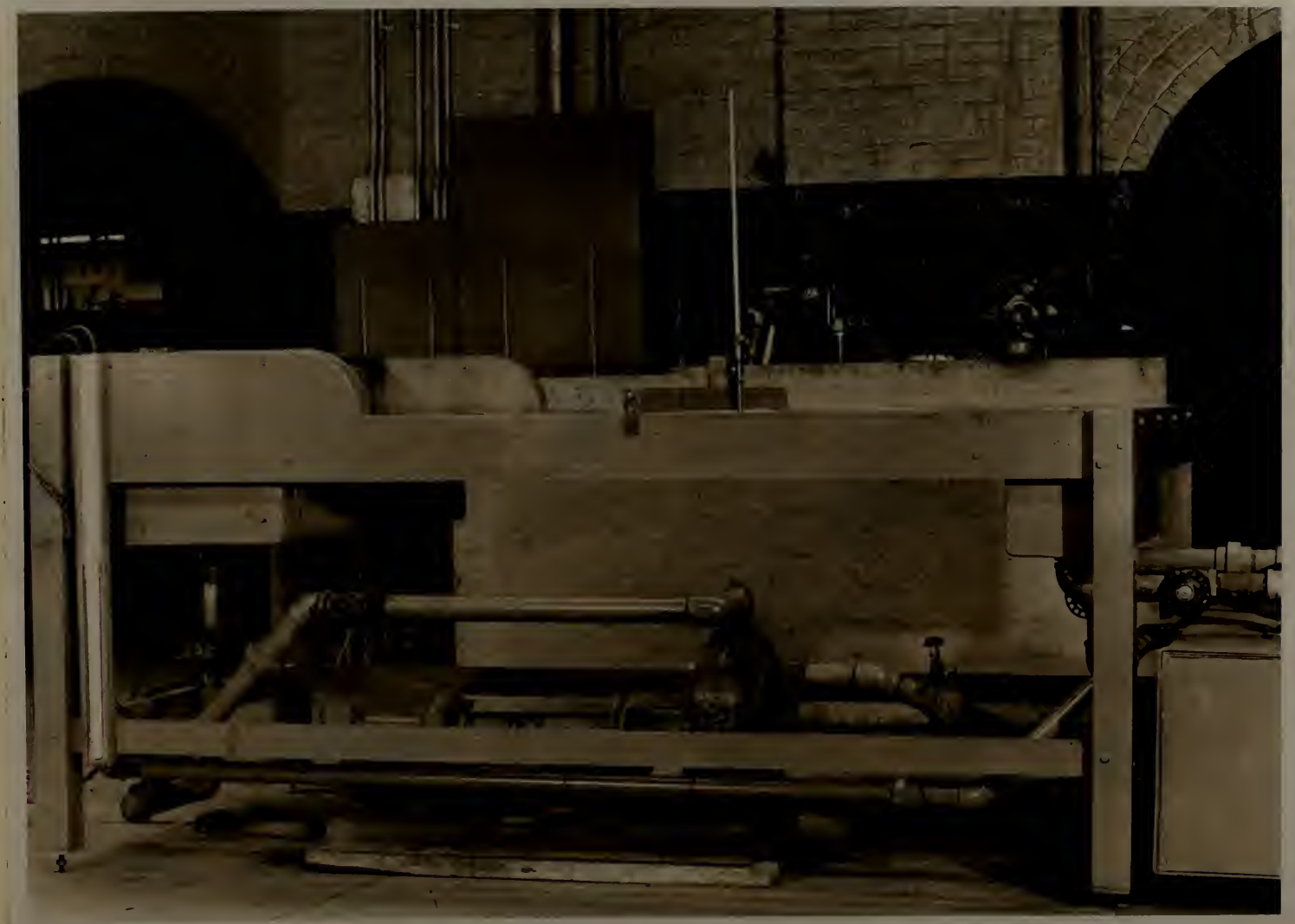

Fig. 10 - WATER TABLE (Side View)

Fig. 11 - WATER TABLE (Top View)

APPENDIX B

Paper No.
46—A-71

Abrupt Energy Transformation in Flowing Gases

By N. P. BAILEY,[1] TROY, N. Y.

After setting up the basic equations of energy, flow, and acceleration, this paper compares theoretical and actual plane compression shocks in tubes. By making the single-plane-angle shock a special case of a plane shock, curves for solving numerical cases are presented. Even though most angle shocks encountered in engineering are three dimensional, it is felt that the simple theory of single-plane shocks is helpful in understanding such phenomena without the complications of three-dimensional theory. Traverses of three-dimensional angle shocks in nozzle and orifice discharges are presented and discussed, and temperature traverses through shock diamonds in high-temperature streams are shown. Although no complete explanation exists for thermocouple readings in excess of the total gas temperature in such high-temperature shocks, their existence is established. As a last case of abrupt energy transformation in gas streams, tests of combustion with flow in a constant-area tube are given. Experiment and analysis agree that the assumptions of constant-area flow and steady or continuous flow do not appear to be simultaneously tenable when combustion is present.

Nomenclature

The following nomenclature is used in the paper:

A = area, sq ft
C_p = specific heat at constant pressure, Btu per lb per deg F
C_v = specific heat at constant volume, Btu per lb per deg F
C_1 = constant of integration
C_2 = constants of integration
d = total differential
∂ = partial differential
F = friction force, lb per ft of length
g = acceleration of gravity; 32.2 fps per sec
H = rate of heat release, Btu per sec per cu ft
J = 778.26 ft-lb per Btu
L = mechanical work, Btu per lb
M = Mach number
P = pressure, psfa
Q = heat added, Btu per lb
R = gas constant; 53.3 for air
T = temperature, deg Rankine (R)
t = time, sec
V = specific volume cu ft per lb
v = velocity, fps
W = weight flow, lb per sec
x = distance, ft
α = deflection angle, deg
γ = ratio of gas specific heats; 1.395 for cold air
θ = shock angle, deg
ρ = mass density, slugs per cu ft

[1] Head, Mechanical Engineering Department, Rensselaer Polytechnic Institute. Mem. A.S.M.E.

Contributed by the Research Committee on Fluid Meters, for presentation at the Annual Meeting, New York, N. Y., December 2–6, 1946, of The American Society of Mechanical Engineers.

Introduction

Mechanical-engineering literature is rich in analytical and experimental information on the continuous, steady flow of gases but there is need for a wider familiarity with gas flow when such discontinuities as compression shocks and combustion with flow are present. The aim of this paper is to present some analytical and experimental information on such discontinuous and intermittent phenomena.

Flow Momentum and Energy Concepts

In any case of flow, such as illustrated in Fig. 1, the difference in the rate at which mass enters and leaves the volume, Adx must be balanced instantaneously by the rate of storage, or

$$\frac{\partial(\rho v A)}{\partial x}\,dx = -A\,dx\,\frac{\partial \rho}{\partial t} \quad \ldots\ldots [1]$$

At any instant the mass of fluid in the volume (Adx) is ($\rho A dx$) and, if it receives a change in velocity

$$dv = \frac{\partial v}{\partial x}\,dx + \frac{\partial v}{\partial t}\,dt \quad \ldots\ldots [2]$$

the acceleration is

$$\frac{dv}{dt} = \frac{\partial v}{\partial x}\frac{dx}{dt} + \frac{\partial v}{dt}\frac{dt}{dt} = v\frac{\partial v}{\partial x} + \frac{\partial v}{\partial t} \quad \ldots\ldots [3]$$

For a wall friction or obstruction force, Fdx, a summation of forces in the flow direction gives

$$-\frac{A\,\partial P}{\partial x}\,dx = F dx - \rho A dx\left[v\frac{\partial v}{\partial x} + \frac{\partial v}{\partial t}\right] = 0 \quad \ldots\ldots [4]$$

A useful relationship may be had by multiplying Equation [1] by v and adding it to Equation (4) to give

$$\frac{A\,\partial P}{\partial x} + \frac{v\partial[\rho A v]}{\partial x} = -(\rho v A)\,\frac{\partial v}{\partial x} - \rho A\left(\frac{\partial v}{\partial t}\right) - F - \frac{A v \partial \rho}{\partial t} \quad \ldots [5]$$

By adding $\left[\frac{P\partial A}{\partial x}\right]$ to both sides of Equation [5] and remembering that $\frac{\partial A}{\partial t} = 0$ for a rigid passage, Equation [5] may be written as

$$P dA - F dx = \frac{\partial[PA + \rho A v^2]}{\partial x}\,dx + \frac{\partial(\rho A v)}{\partial t}\,dx \quad \ldots\ldots [6]$$

For the usual steady-flow case where $\frac{\partial(\rho A v)}{\partial t} = 0$, Equation [6] says that the net wall force on the gas in the direction of flow is

$$P dA - F dx = d\,[PA + \rho A v^2] \quad \ldots\ldots [7]$$

1-48 Discussion on this paper will be accepted until February 3, 1947

where $[PA + \rho Av^2]$ is the total momentum per second in pounds passing any section.

Since $\left[\rho = \frac{P}{gRT}\right]$ and the Mach number $\left[\mathbf{M} = \frac{v}{\sqrt{\gamma gRT}}\right]$ it is often convenient to express Equation [7].

$$\text{Net wall reaction} = PdA - Fdx = d\,[PA(1 + \gamma \mathbf{M}^2)] \ldots [8]$$

This statement is true only so long as the flow is steady and it does not hold when the mass flow (ρAv) changes with time. However, since any such flow variation must go through a repeated cycle, the average value of $\int d(\rho Av)$ must be zero and Equation [7] may be used to evaluate the average wall force even when the flow is unsteady or intermittent. This point will be covered by experimental work later.

As gas flows along a channel as in Fig. 1, any thermal energy

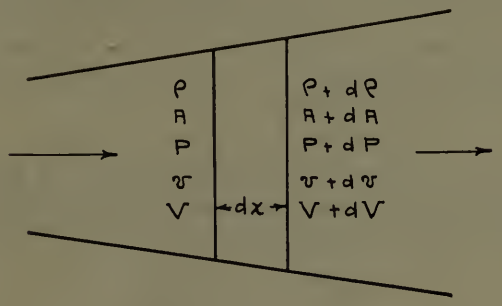

FIG. 1

(dQ) that is released or added, and any work done on it (dL), as in a compressor impeller, must be accounted for. Some of it will go to change the internal energy ($C_v dT$) and part to do flow work $\left(\frac{VdP}{J}\right)$ as the gas flows through a pressure change. With a pressure change (dP), a compressible gas will undergo a volume change (dV), and do an amount of expansion work $\left(\frac{PdV}{J}\right)$ and an increase in velocity would induce a kinetic-energy change $\left(\frac{1}{Jg} vdv\right)$.

This results in an energy-balance equation

$$dL + dQ = C_v dT + \frac{1}{J} VdP + \frac{1}{J} PdV + \frac{1}{Jg} vdv \ldots [9]$$

A reversible process is characterized by $dQ = 0$ and

$$C_v dT + \frac{1}{J} PdV = 0 \ldots [10]$$

Such a process is thus defined as one where the only internal energy change is the inevitable one resulting from compression or expansion work.

A useful form of the energy equation for general applications is

$$dL + dQ = \frac{\gamma}{(\gamma - 1)} \frac{R}{J} dT + \frac{1}{Jg} vdv \ldots [11]$$

For the case of constant total energy ($dL = 0$ and $dQ = 0$), if Equation [11] is integrated between any velocity v, and corresponding static temperature T, and a final velocity of zero where the static temperature is the same as the total temperature T_o, the result is

$$\gamma gRT + \frac{(\gamma - 1)}{2} v^2 = \gamma gRT_o \ldots [12]$$

When this is combined with the Mach number definition

$$\mathbf{M}^2 = \frac{v^2}{\gamma gRT} \ldots [13]$$

The result is

$$T_{(\text{static})} = \frac{T_{o(\text{total})}}{1 + \frac{(\gamma - 1)}{2} \mathbf{M}^2} \ldots [14]$$

For the case of steady flow

$$W = \rho gAv \ldots [15]$$

and this combined with the gas equation and with Equations [13] and [14] gives

$$\frac{W\sqrt{T_0}}{AP} = \mathbf{M} \sqrt{\frac{\gamma g}{R}\left[1 + \frac{(\gamma - 1)}{2} \mathbf{M}^2\right]} \ldots [16]$$

Equation [16] is very useful in all cases of steady flow at constant total energy.

PLANE SHOCKS

For the simple case of steady flow at constant area and constant total energy with no appreciable wall friction, Equation [8] becomes

$$P(1 + \gamma \mathbf{M}^2) = P_1(1 + \gamma \mathbf{M}_1^2) = P_2(1 + \gamma \mathbf{M}_2^2) = \text{const} \ldots [17]$$

and Equation [16] may be written

$$P\mathbf{M}\sqrt{1 + \frac{(\gamma - 1)}{2} \mathbf{M}^2} = P_1\mathbf{M}_1\sqrt{1 + \frac{(\gamma - 1)}{2} \mathbf{M}_1^2} = P_2\mathbf{M}_2\sqrt{1 + \frac{(\gamma - 1)}{2} \mathbf{M}_2^2} = \text{const} \ldots [18]$$

When (P_2/P_1) is eliminated between Equations [17] and [18], one obvious solution for the equation of constant area and constant total energy flow without friction is for $(\mathbf{M}_1 = \mathbf{M}_2)$, but when this root $(\mathbf{M}_2 - \mathbf{M}_1)$ is factored out, the result is

$$\mathbf{M}_2^2 = \frac{1 + \frac{(\gamma - 1)}{2} \mathbf{M}_1^2}{\gamma \mathbf{M}_1^2 - \frac{(\gamma - 1)}{2}} \ldots [19]$$

and

$$P_2/P_1 = \frac{2\gamma \mathbf{M}_1^2 - (\gamma - 1)}{(\gamma + 1)} \ldots [20]$$

This means that for any superacoustic Mach number $\mathbf{M}_1$, there is a subacoustic Mach number $\mathbf{M}_2$, which satifies the conditions of flow. This defines a plane compression shock which is a discontinuity, occurring theoretically in an extremely short distance. Whether or not it will occur in any case depends upon operation conditions. Since channel friction[2] causes superacoustic flow to approach the acoustic, for any initial Mach number there is a maximum flow distance for which shockless flow is possible.

A shock may also be induced in a shorter channel by applying the correct back pressure. For any initial Mach number and channel friction, each position of the shock uniquely determines one back pressure. This is illustrated in Fig. 2, where $A - 1 - B$ represents flow that is all superacoustic. If the back pressure

[2] "The Thermodynamics of Air at High Velocities," by N. P. Bailey, *Journal of the Aeronautical Sciences*, vol. 11, July, 1944, p. 227.

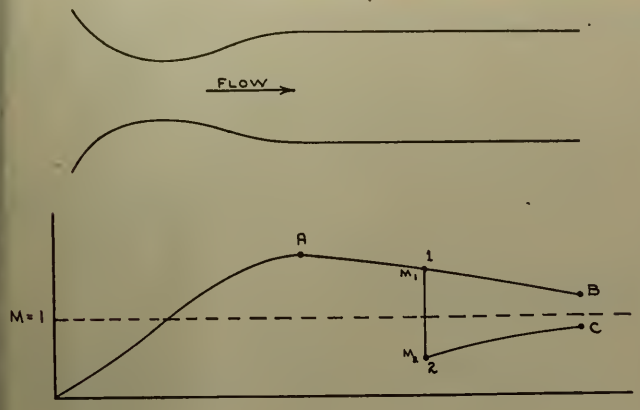

FIG. 2

is raised somewhat, the flow adjusts to it by a plane compression shock at some point 1, going to subacoustic flow at 2, and discharging subacoustically at C. Equation [19] indicates that the Mach number after shock approaches $\sqrt{\frac{(\gamma-1)}{2\gamma}}$ as M_1 becomes very large, and it cannot go below that value.

The magnitudes of the pressure rise and Mach number change of actual compression shocks check well[2] with theoretical values from Equations [19] and [20]. However, instead of being completed in a negligible distance, the pressure rise extends over a distance of from one to five pipe diameters.

This is illustrated by the test data shown in Fig. 3. Both wall and center pressure traverses were taken for the conditions shown

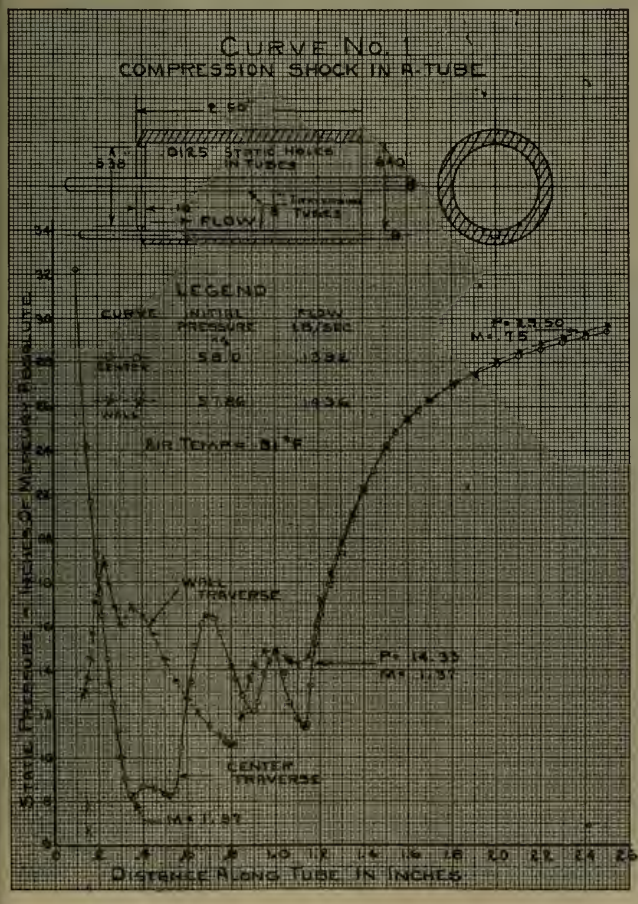

FIG. 3 COMPRESSION SHOCK IN A TUBE

and after a series of angle shocks in the first 1.15 in. of the tube, the wall and center pressures became the same, and a plane compression shock was initiated. The Mach number as calculated from Equation [16] for an initial pressure of 14.33 in. of mercury was $M_1 = 1.37$. Similarly at the final pressure of 29.50 in., M_2 was 0.75. From Equation [19], a shock, started at $M_1 = 1.37$, should have ended at $M_2 = 0.748$, and from Equation [20] the pressure should be $P_2 = 29.50$.

The only discrepancy lies in the fact that the pressure rise is distributed over a length of 1.3 in. instead of being an abrupt change as illustrated in Fig. 2. The explanation of this lies in the effect of boundary layer and the use of a manometer to measure pressure. Since the flow in the boundary layer is subacoustic, no compression shock and corresponding pressure rise can occur in it. This means that at any instant the large pressure rise across the shock front is short-circuited through the boundary layer. This immediately causes the shock to collapse and form at some other point, only to collapse again. Since the manometer reading is a time average of the pressure at any point, a value of one half the pressure rise, occurring at 1.4 in., Fig. 3, merely means that the compression shock is upstream from that point one half the time and downstream from there the other half of the time. The shock is constantly dancing back and forth in the tube, never being further upstream than the 1.17-in. point and never further downstream than 2.5 in.

This explanation is borne out by high-speed photography, as well as by the fact that an open-end impact tube tunes to a shrill whistle in such a shock region. Consequently, the simple picture of Fig. 2 will have to be modified to show the compression shock (1–2) as sweeping back and forth in the tube through a distance that varies with boundary-layer thickness, tube size, and initial Mach number.

ANGLE SHOCKS

When supersonic gas flow encounters an obstruction which calls for it to change its flow direction, an angle shock will occur. This is because the approach velocity is so high that the first molecules to find themselves in trouble are not capable of sending a distress signal upstream. This means that each successive layer of gas molecules must run into the same trouble with no warning.

This is illustrated in Fig. 4 for the simple two-dimensional case where supersonic parallel flow at a velocity v_1, must turn through an angle α, and flow parallel in a new direction. This entire change takes place in a shock front at an angle θ, from the original flow direction. Such an angle shock may be made into a special case of the plane shock, discussed previously, by viewing it as a normal velocity ($v_1 \sin\theta$), going through a plane shock to a velocity v_2', and this all occurring in a flow field having a uniform velocity ($v_1 \cos\theta$) parallel to the shock front. This can be done

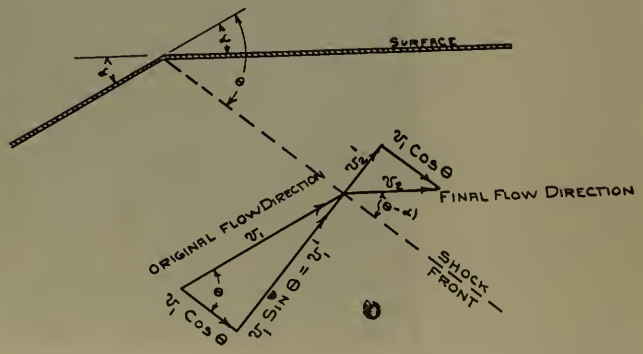

FIG. 4

because there is a pressure rise normal to the shock front but no pressure gradient to give a velocity change parallel to the shock front.

From Fig. 4 the condition that the normal component of the velocity must be reduced to a value v_2', that will cause the final velocity v_2, to be turned through an angle α, may be stated as

$$\frac{v_2'}{v_1 \cos\theta} = \tan(\theta - \alpha) \quad \ldots\ldots [21]$$

From Equations [13] and [14]

$$v_1 \cos\theta = \frac{\sqrt{\gamma g R T_{o1}}\, M_1 \cos\theta}{\sqrt{1 + \frac{(\gamma-1)}{2} M_1^2}} \quad \ldots\ldots [22]$$

Also, since $v_1' = v_1 \sin\theta$, for the same static temperature $T_1 = T_1'$, Equation [13] says that

$$M_1' = M_1 \sin\theta \quad \ldots\ldots [23]$$

From Equation [19] then

$$M_2'^2 = \frac{1 + \frac{(\gamma-1)}{2} M_1'^2}{\gamma M_1'^2 - \frac{\gamma-1}{2}} = \frac{1 + \frac{(\gamma-1)}{2} M_1^2 \sin^2\theta}{\gamma M_1^2 \sin^2\theta - \frac{(\gamma-1)}{2}} \quad \ldots [24]$$

Before (v_2') can be evaluated from Equations [22] and [24], the total temperature $T_{o2}' = T_{o1}'$ must be expressed. The static temperature $T_1' = T_1$ may be evaluated from Equation [14] as

$$T_1 = T_1' = \frac{T_{o1}}{1 + \frac{(\gamma-1)}{2} M_1^2} \quad \ldots\ldots [25]$$

Since, from Equation [22]

$$v_1' = v_1 \sin\theta = \frac{\sqrt{\gamma g R T_{o1}}\, M_1 \sin\theta}{\sqrt{1 + \frac{(\gamma-1)}{2} M_1^2}} \quad \ldots\ldots [26]$$

and from Equation [12] the total temperature T_{o1}' is

$$T_{o1}' = T_{o2}' = T_1' + \frac{(\gamma-1)}{2\gamma g R} v_1'^2 \quad \ldots\ldots [27]$$

This gives the total temperature T_{o2}' as

$$T_{o2}' = \frac{T_{o1}}{1 + \frac{(\gamma-1)}{2} M_1^2} + \frac{(\gamma-1)\, T'_{o1}\, M_1^2 \sin^2\theta}{2\left[1 + \frac{(\gamma-1)}{2} M_1^2\right]} \quad \ldots [28]$$

Using Equations [24] and [28' in

$$v_2' = \frac{\sqrt{\gamma g R T_{o2}'}\, M_2'}{\sqrt{1 + \frac{(\gamma-1)}{2} M_2'^2}} \quad \ldots\ldots [29]$$

gives

$$v_2' = \frac{\sqrt{\gamma g R T_{o1}}}{\sqrt{1 + \frac{(\gamma-1)}{2} M_1^2}} \cdot \frac{\left[1 + \frac{(\gamma-1)}{2} M_1^2 \sin^2\theta\right]}{\frac{(\gamma+1)}{2} M_1 \sin\theta} \quad \ldots [30]$$

From Equations [30] and [22] in [21]

$$\tan(\theta - \alpha) = 4 \frac{\left[1 + \frac{(\gamma-1)}{2} M_1^2 \sin^2\theta\right]}{(\gamma+1) M_1^2 \sin 2\theta} \quad \ldots\ldots [31]$$

Equation [31] defines the shock angle θ for gas flow at an initial Mach number M_1, being deflected through an angle α.

Using $M_1' = M_1 \sin\theta$ in Equation [20] gives the static-pressure-ratio rise through the single-plane-angle shock as

$$\frac{P_2}{P_1} = \frac{2\gamma M_1^2 \sin^2\theta}{(\gamma+1)} - \frac{(\gamma-1)}{(\gamma+1)} \quad \ldots\ldots [32]$$

The resultant final velocity v_2 is given by

$$v_2 = \sqrt{v_2'^2 + v_1^2 \cos^2\theta} \quad \ldots\ldots [33]$$

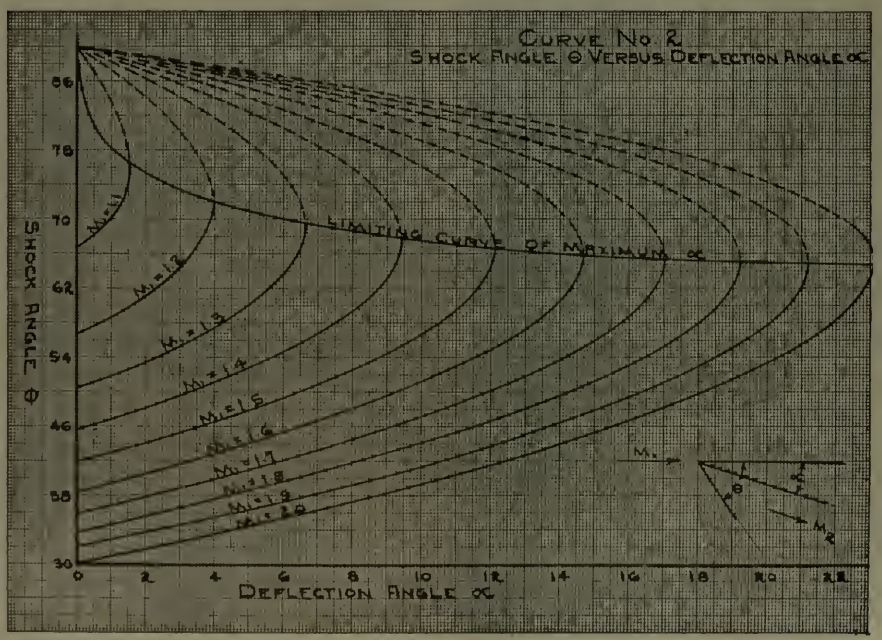

FIG. 5 SHOCK ANGLE θ VERSUS DEFLECTION ANGLE α

Using Equation [21] for v_2' and Equation [22] for $v_1 \cos\theta$ in Equation [33]

$$v_2 = \frac{\sqrt{\gamma g R T_{o1}}\, M_1 \cos\theta}{\sqrt{1 + \frac{(\gamma-1)}{2} M_1^2 \cos(\theta - \alpha)}} \quad \ldots\ldots [34]$$

From Equations [12] and [13]

$$M_2 = \frac{1}{\sqrt{\frac{\gamma g R T_{o2}}{v_2^2} - \frac{(\gamma-1)}{2}}} \quad \ldots\ldots [35]$$

Since v_1 and v_2 are total velocities and a compression shock is at constant total energy, $T_{01} = T_{02}$

$$M_2 = \frac{1}{\sqrt{\frac{\left[1 + \frac{(\gamma-1)}{2} M_1^2\right] \cos^2(\theta - \alpha)}{M_1^2 \cos^2\theta} - \frac{(\gamma-1)}{2}}} \quad \ldots [36]$$

This gives the final Mach number M_2, after an angle shock from an initial value of M_1, when single-plane flow is deflected through an angle α.

Fig. 5 shows values of shock angle θ, plotted against the deflection angle α, for various values of initial Mach number as calculated from Equation [31]. For each value of M_1 there is a maximum deflection angle for which angle shock conditions can be satisfied and for any increased deflection angle a plane shock will result. This maximum point represents the conditions where a wedge in a free stream would cease to have angle shocks from its nose and would have a bow shock out in front of it.

Fig. 6 shows corresponding values of shock-pressure ratio for various conditions, and Fig. 7 shows the final Mach number after an angle shock. Whereas the flow after a plane shock is always subacoustic, it may be either above or below sonic in the case of angle shocks.

When supersonic air flows past a wedge, the angle shocks are stably anchored at the nose of the wedge, but when a boundary layer is present, the shock pressure rise is distributed over an appreciable distance as in the case of a plane shock.

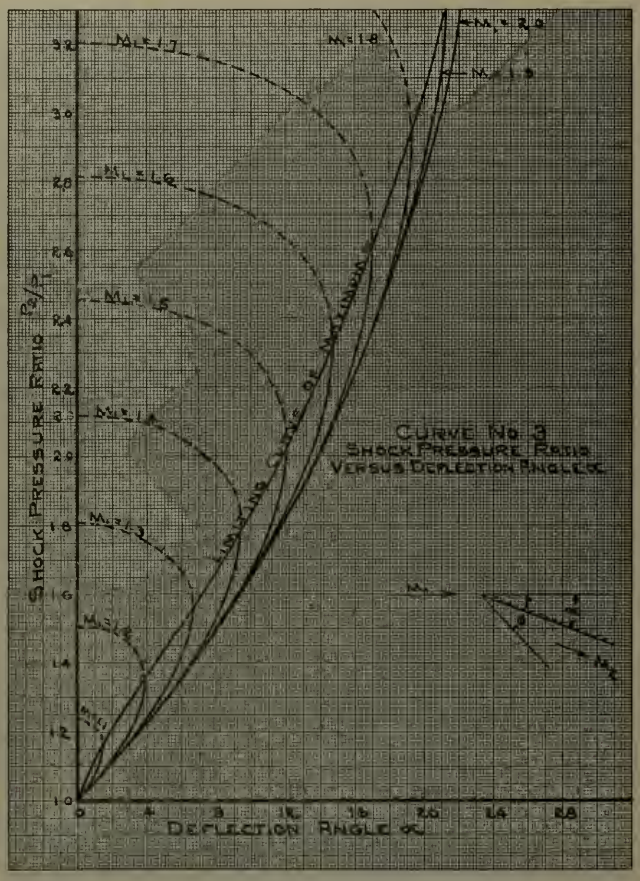

Fig. 6 Shock-Pressure Ratio Versus Deflection Angle α

In Fig. 3, where the first angle shock originated at the wall, the pressure rise extended from 0.14 in. to 0.22 in. The first pressure rise indicated by the center traverse spread between 0.56 in. and 0.72 in. In the next angle shock at the wall where the boundary layer was thicker, the pressure rise extended from 0.80 in. to 0.95 in. This would indicate that angle shocks emanating from a channel wall are unstably anchored to a subsonic boundary layer the same as plane shocks.

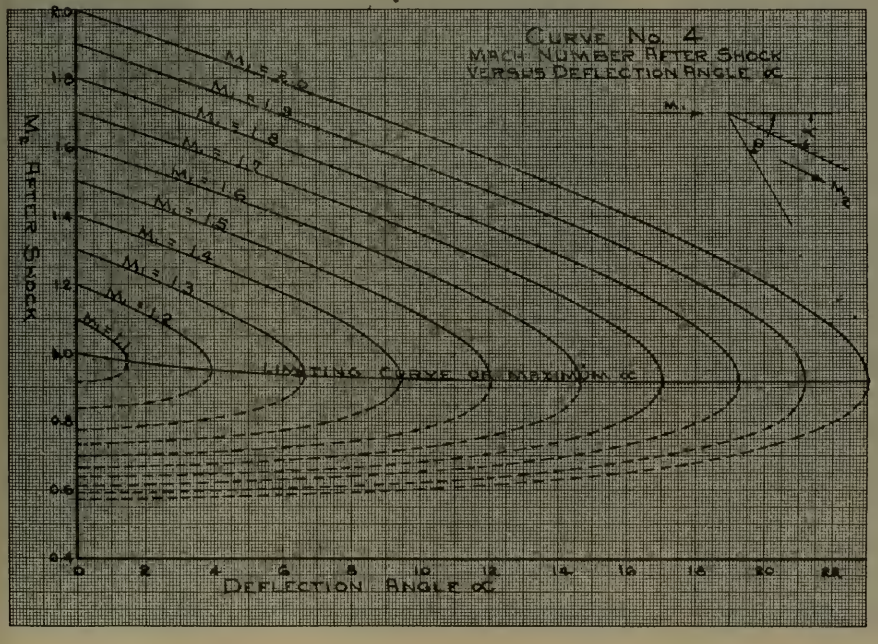

Fig. 7 Mach Number After Shock Versus Deflection Angle α

Shocks at High Temperatures

When a gas flows through an orifice or a parallel-walled nozzle under a pressure ratio greater than that needed to produce sonic velocity, the sudden adjustment of the gas pressure to the lower back pressure produces a variety of angle shock patterns. Fig. 8 shows static and impact pressure center traverses for such flow from a simple nozzle, together with the probable shock and rare-faction wave pattern.

The fact that each pressure rise is spread over a distance of 0.15 in. indicates that, owing to the boundary layer

in the nozzle, the shock pattern was not stable and stationary in space. Further evidence of such instability was furnished by the whistling of the impact tube in the region from 0.05 in. inside the nozzle to 0.10 in. outside of it.

The loss of impact pressure and the subsequent recovery of it between 0.15 and 0.40 in. marks the region where the flow was sufficiently supersonic to produce a serious shock in front of the impact tube. The distance of this shock bow in front of the impact tube appears to have been about 0.08 in.

It is usually assumed that the first angle compression shock emanates from the nozzle wall, but the traverse of the jet from an orifice, shown in Fig. 9, indicates that angle compression shocks can originate from a jet boundary. Sonic velocity was not reached until 0.2 in. from the orifice and no disturbance reached the center traversing tube in the first 0.33 in. At that point an angle shock and the subsequent rarefaction were followed by a plane or bow shock in front of the tube shown in the stream.

Such shock patterns as shown by the curves in Figs. 8 and 9, respectively, are quite common, and alternate compressions and rarefactions usually persist for 6 or more oscillations before they are damped out. With low-temperature gases, they are detectable only by making pressure traverses or by schlerin photographs.

When these shock patterns occur in high-temperature products of combustion, the high-pressure-shock diamonds are directly visible and are usually a beautiful blue color. Such a view is illustrated in Fig. 10. Fig. 11 shows test results for thermocouple readings taken in such a shock region in a stream of products from an orifice approximately 2 in. diam. The first reaction to such results as shown in Fig. 11 is that of utter disbelief. However, the chance of unusual instrumentation errors has been systematically eliminated by repeating such test runs under a variety of conditions, always with the same results.

The next idea is that there is unburned fuel being discharged from the orifice, which burns on the surface of the thermocouple and produces a local temperature rise. The chance of this being the case is very small for two reasons: (*a*) The original burner temperature checks a heat balance on the air and fuel supplied within 2 per cent; (*b*) the appearance and color of the shock diamonds are not at all altered by the insertion of a thermocouple.

Another possible explanation is that some unstable oxides of nitrogen are formed in the region of shock where there are rates of deceleration greater than 2,000,000 g. This again has been eliminated by burning propane with pure oxygen and observing exactly the same phenomenon.

Fig. 12 indicates that it is a phenomenon definitely associated with shocks. The data for the curves in Figs. 12 and 13, respectively, were taken in a $^{3}/_{16}$-in. jet with a fairly large thermocouple ($^{1}/_{8}$-in. sheath), so the cooling effect was quite pronounced. As a result, the excess temperatures shown are much smaller than those shown for the large jet in Fig. 10, but they are more analytical.

Fig. 12 indicates further that this phenomenon is definitely geared to the strength of the compression shock, for it completely disappears at orifice or burner pressure ratios where shocks are not present. It would naturally be expected that an unshielded thermocouple in a small stream of hot gases would

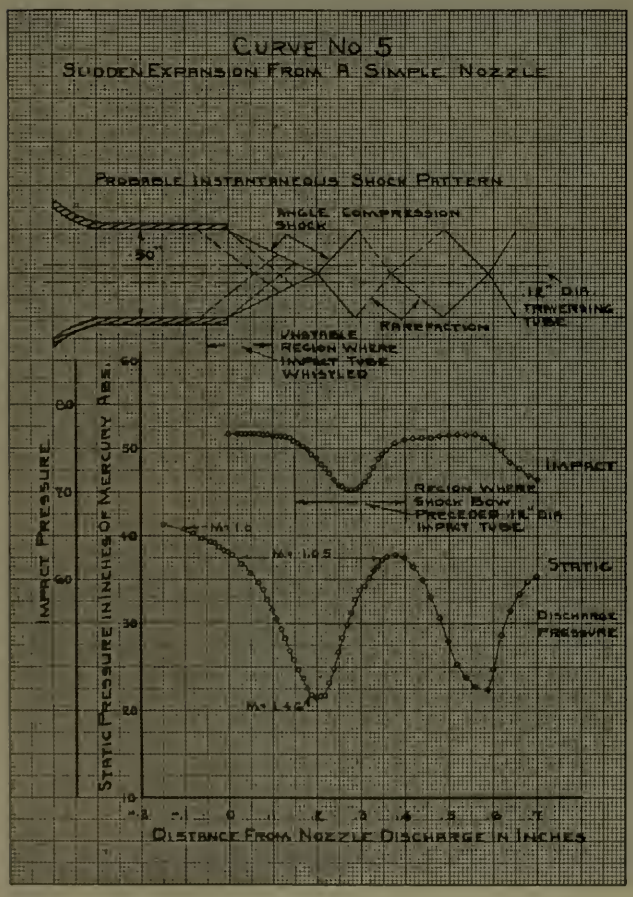

FIG. 8 SUDDEN EXPANSION FROM A SIMPLE NOZZLE

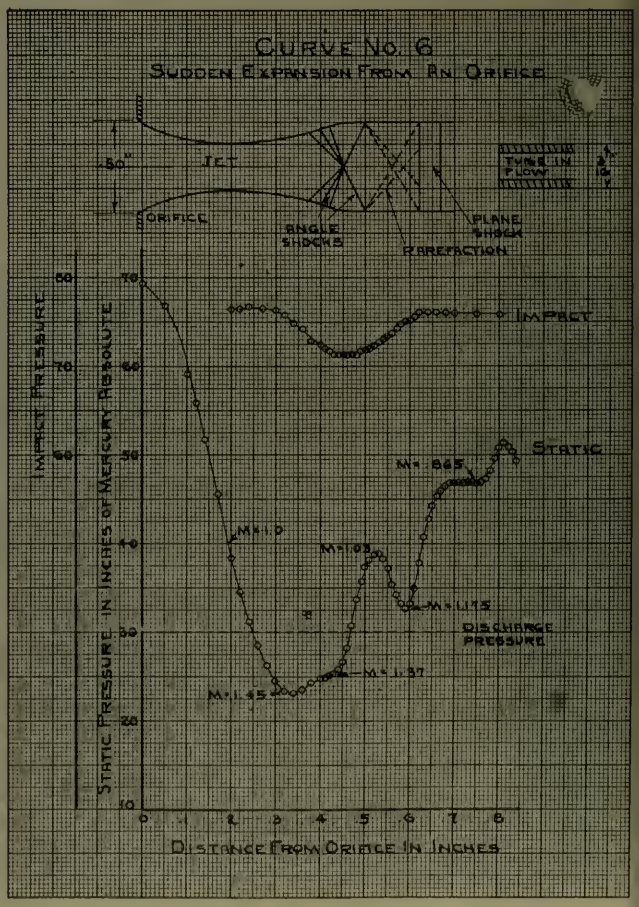

FIG. 9 SUDDEN EXPANSION FROM AN ORIFICE

Fig. 10 High-Pressure-Shock Diamonds in High-Temperature Products of Combustion

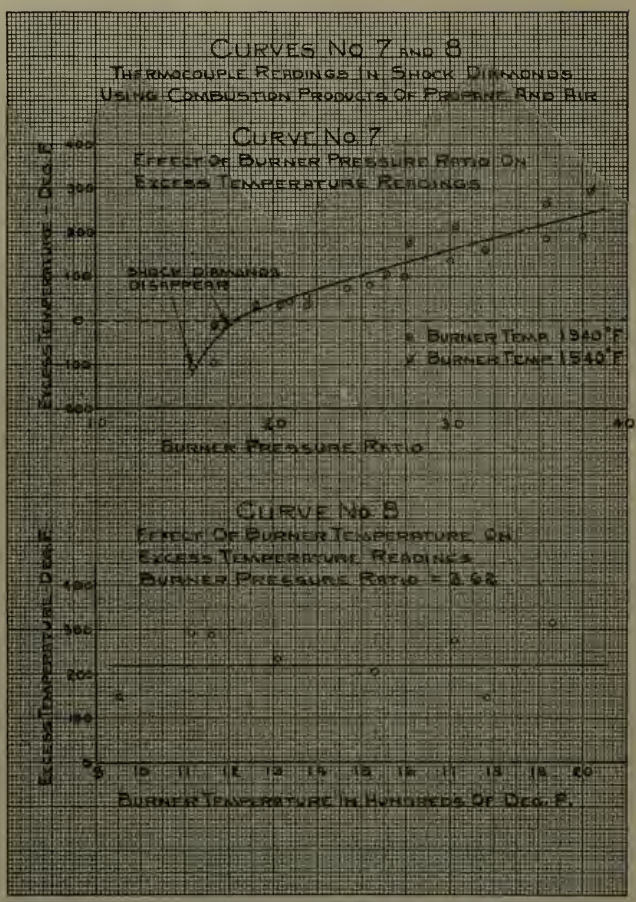

Fig. 12 (*Above*) Thermocouple Readings in Shock Diamonds Using Combustion Products of Propane and Air: Effect of Burner Pressure Ratio on Excess Temperature Readings

Fig. 13 (*Below*) Thermocouple Readings in Shock Diamonds Using Combustion Producers of Propane and Air: Effect of Burner Temperature on Excess Temperature Readings, Burner Pressure Ratio = 3.62

read from 100 to 200 deg F low owing to radiation losses and velocity errors, and that is what happened below pressure ratios of 1.9.

Fig. 13 indicates that within the limits of accuracy of the test data, the amount of excess temperature is fairly independent of burner temperature above 1100 F. No test data are available for initial temperatures between 1100 F and 80 F. However, repeated attempts to find excess thermocouple readings in shocks at a temperature at 80 F failed.

Since the thermocouple metal reaches a temperature greater than the total temperature of the gas before it is in energy equilibrium, it is evident that it is being bombarded by something besides gas molecules. The violent deceleration of the hot gases in the shock could produce such a high concentration of ions that their bombardment and neutralization at the thermocouple metal surface could cause the metal to reach a very high temperature before energy equilibrium

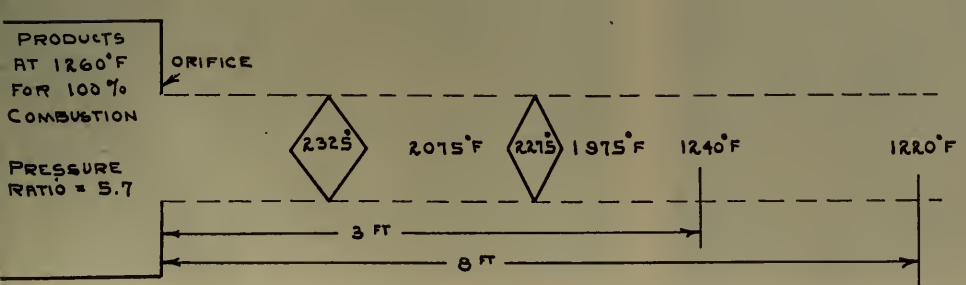

Fig. 11

is reached. This phenomenon deserves a thorough investigation.[3]

Combustion and Flow

Combustion of air-fuel mixtures is customarily done with no appreciable flow velocity and too little is known of the mechanism involved when combustion occurs in a high-velocity air stream. The most commonly discussed case of combined combustion and flow is that of burning in a constant-area passage which is such a short distance that wall friction forces may be neglected.

If it is also assumed that the area is constant and the flow is steady, Equation [7] gives the condition for constant momentum per second as

$$P_1 + \rho_1 v_1^2 = P_2 + \rho_2 v_2^2 \ldots\ldots\ldots\ldots [37]$$

solving for the increase in velocity pressure

$$\frac{\rho_2 v_2^2}{2} - \frac{\rho_1 v_1^2}{2} = \frac{P_1 - P_2}{2} \ldots\ldots\ldots\ldots [38]$$

This says that the gain in velocity pressure is only one half the drop in static pressure. It was to find out, if possible, how the gas stream goes about losing the rest of this static pressure without wall friction that the following tests were made:

The $1^3/_8$-in-diam thin-walled tube, used in Figs. 14 and 15, was lined up axially in the air stream from a 3-in-diam nozzle. Hydrogen for heating was introduced through the $^3/_8$-in-diam tube shown. By regulating the size and arrangement of hydrogen jets and the hydrogen pressure, a uniform temperature could be reached across the entire cross section. Static and total pressures was obtained with $^1/_{10}$-in. traversing tubes, and temperatures with an unshielded thermocouple of the same maximum diameter. All values shown represent averages of the annulus around the hydrogen tube.

In general, two quite different sets of conditions could be obtained. When the heating was uniform across the tube the results in Fig. 14 are representative of several tests. The burning was a series of explosions at the resonant frequency of the tube. This frequency was high enough for manometers and thermocouples to give steady readings, but it was a violently noisy form of combustion. The thing which characterizes these results shown in Fig. 14 is that the velocity pressure $\left(\frac{\rho v^2}{2}\right)$ increases in the region where the temperature is rising.

However, when the hydrogen tube was placed slightly off center and the tube wall became a bit hotter on one side, the combustion became anchored and was very quiet and orderly. The traverses in Fig. 15 are typical of these tests, and they are characterized by the fact that practically all of the velocity-pressure increase occurred ahead of the temperature rise. The chief loss in total pressure occurred in the burning region where the velocity pressure remained essentially constant.

This would indicate some form of jet separation in the tube ahead of the combustion, followed by combustion at essentially constant velocity pressure as the flow again filled the tube. Fig. 16 shows the velocity plotted against absolute temperature and for the tube to flow full, the velocity would be essentially proportional to temperature, that is, if the weight of hydrogen

[3] Such a program is being carried on by the Mechanical Engineering and Physics Departments of the Rensselaer Polytechnic Institute.

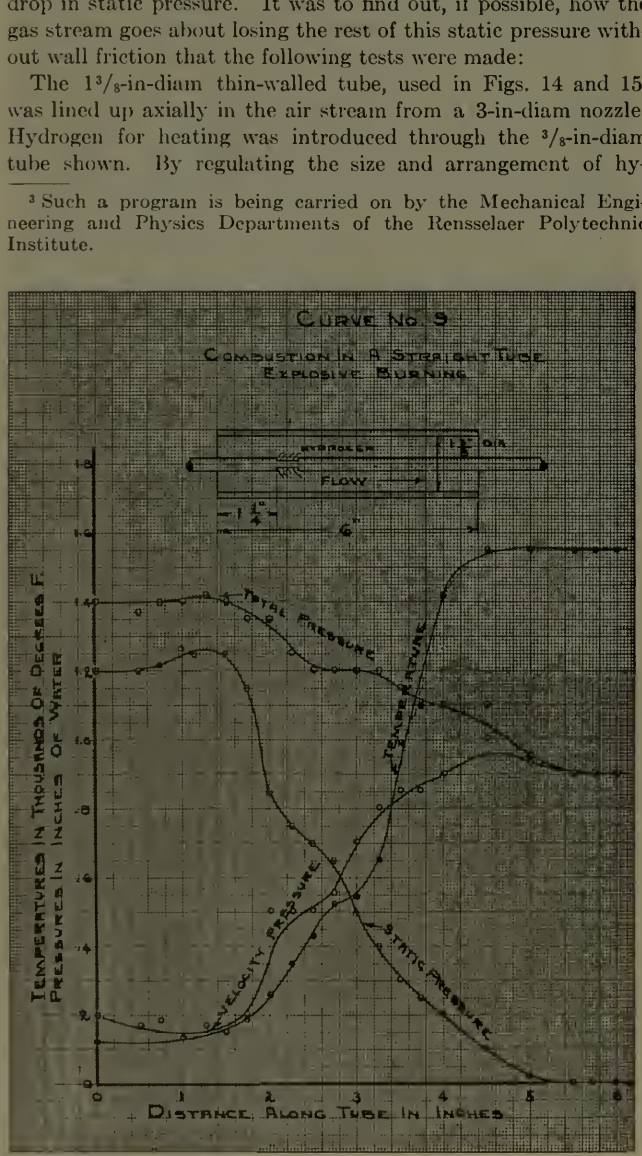

Fig. 14 Combustion in Straight Tube; Explosive Burning

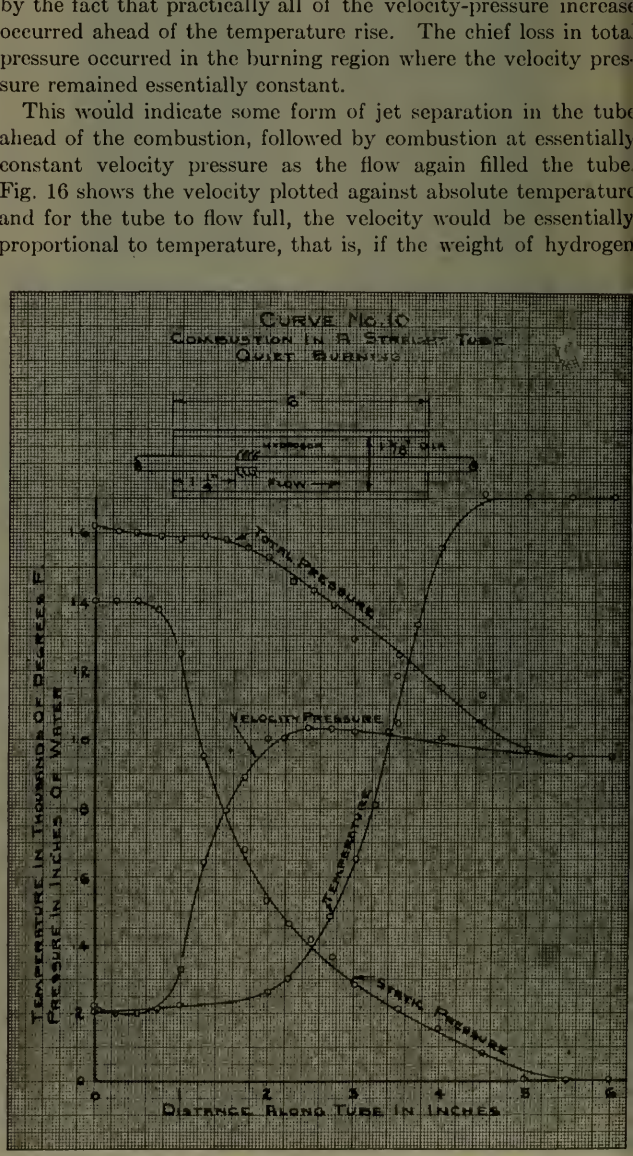

Fig. 15 Combustion in Straight Tube; Quiet Burning

added and the small pressure change are neglected. The points before and after combustion do lie very close to such a line, but the velocity in the burning region is much higher. This furnishes a good indication that the tube was not flowing full.

In the second section of the paper it was concluded that even with unsteady flow, Equation [33] would be true for averaged readings. For the case of the curve in Fig. 14, for intermittent flow and explosive burning, the ratio of velocity-pressure increase to static-pressure decrease was 0.65 instead of the theoretical 0.50. In the steady-flow case in Fig. 15 it was 0.57, and for another series of eight tests it varied from 0.52 to 0.58. Since Equation [38] does not account for the addition of hydrogen to the flowing gas stream this is not a bad check.

It is easy to assume that just because combustion occurs in a constant-area tube the burning occurs at constant area. The limited amount of test work at hand would seem to cast doubt on the validity of the simultaneous assumptions of steady flow and constant-area combustion.

Some of the implications of these assumptions may be had by assuming a rate of heat release of H Btu per sec per cu ft of volume, and stating that for steady operation an amount of energy $AHdx$ must be transported out of the volume Adx, each second; or, from the energy equation

$$HAdx = WC_p dT + \frac{W}{Jg} vdv \quad \ldots\ldots [39]$$

For acceleration, with no wall friction

$$AdP = -\rho Adx \frac{dv}{dt} = -\rho Avdv = -\frac{W}{g} dv \quad \ldots\ldots [40]$$

For steady flow

$$W = \rho Agv = \frac{P}{RT} Av \quad \ldots\ldots [41]$$

Integrating Equation [40]

$$AP = -\frac{W}{g} v + C_1 \quad \ldots\ldots [42]$$

For any initial condition P_1 and v_1, C_1 may be evaluated to give

$$v = v_1 + \frac{Ag}{W} (P_1 - P) \quad \ldots\ldots [43]$$

From Equations [40] and [43]

$$vdv = -\frac{gA}{W} dP \left[v_1 + \frac{Ag}{W} (P_1 - P) \right] \quad \ldots\ldots [44]$$

Differentiating Equation [41]

$$dT = \frac{A}{RW} d(Pv) = \frac{A}{RW} vdP + \frac{A}{RW} Pdv \quad \ldots\ldots [45]$$

From Equations [40], [43], and [45]

$$dT = \frac{A}{RW} dP \left[v_1 + \frac{Ag}{W} (P_1 - P) \right] - \frac{gA^2 PdP}{RW^2} \quad \ldots [46]$$

From Equations [44] and [46] in [39].

$$\frac{dP}{dx} = \frac{HW}{gA \left\{ \left(\frac{C_p}{R} - \frac{1}{J} \right) \left[\frac{Wv_1}{Ag} + (P_1 - P) \right] - \frac{C_p}{R} P \right\}} \quad \ldots [47]$$

Since, from Equation [41]

$$Wv_1 = W_1 v_1 = \frac{P_1 A}{RT_1} v_1^2 \quad \ldots\ldots [48]$$

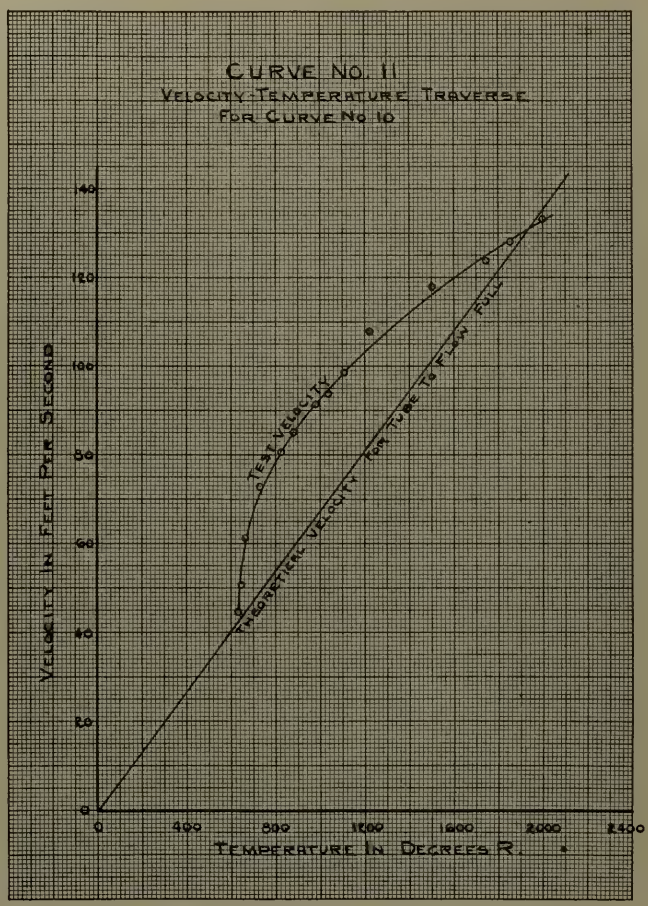

FIG. 16 VELOCITY-TEMPERATURE TRAVERSE FOR CURVE, FIG. 15

and from definition

$$\frac{v_1^2}{\gamma g R T_1} = M_1^2 \quad \ldots\ldots [49]$$

and

$$\frac{C_p}{R} - \frac{1}{J} = \frac{C_v}{R} = \frac{1}{J(\gamma - 1)} \quad \ldots\ldots [50]$$

Equations [48], [49], and [50] with Equation [47] given

$$\frac{dP}{dx} = -\frac{HJW(\gamma - 1)}{P_1 gA} \left[\frac{1}{(\gamma + 1) \frac{P}{P_1} - (\gamma M_1^2 + 1)} \right] \quad \ldots [51]$$

This type of a pressure gradient has all the earmarks of instability, for (dP/dx) becomes a greater negative value as P becomes smaller. This would indicate that the effect would tend to cumulate until (dP/dx) becomes minus infinity which would be a discontinuous front. Consequently, analysis appears to bear out the experimental conclusion that true constant-area burning cannot also be a steady-flow phenomenon.

ACKNOWLEDGMENTS

The author wishes to give due credit to Profs. Harold A. Wilson and Frederick J. Bordt of Rensselaer Polytechnic Institute for assistance, and to acknowledge that he did much of the experimental work while in the research laboratory at the General Electric Company.

Printed in U.